Kinetics of the Reaction of Hydroxyl Radicals with Ethane and a Series of Cl- and F-substituted Methanes at 300-400 K. OH as a Tropospheric Sink Preventing Ozone Depletion

Bjarnov, E.; Munk, J.; Nielsen, Ole John; Pagsberg, Palle Bjørn

Publication date:
1983

Document Version
Publisher's PDF, also known as Version of record

RISØ-M-2366

KINETICS OF THE REACTION OF HYDROXYL RADICALS WITH ETHANE AND A SERIES OF Cl- AND F-SUBSTITUTED METHANES AT 300-400°K. OH AS A TROPOSPHERIC SINK PREVENTING OZONE DEPLETION

Contract No. 180.21-2.4 NORDISK MINISTERRÅD

Erik Bjarnov, Jette Munk, Cle John Nielsen,
Palle Pagsberg, and Alfred Sillesen

Abstract. Gas phase reactions of hydroxyl radicals with ethane and a series of Cl- and F-substituted methanes were studied at atmospheric pressure and over the temperature range 300-400°K. Hydroxyl radicals were produced by pulse radiolysis of water vapour and the decay rate was studied by monitoring the transient light absorption at 3090 A. Arrhenius parameters (A, E_a) for the reaction RH + OH -> R + HOH were obtained for the reactants RH = C_2H_6, CH_3Cl, CH_2Cl_2, $CHFCl_2$. CF_2Cl_2 (CFC-12) which contains no C-H bonds was found to be inert toward attack by hydroxyl radicals. Since no other tropospheric sink reactions have been reported for CFC-12 its possible impact on the stratospheric ozone remains a controversial problem.

→

INIS-descriptors: AIR POLLUTION; CHEMICAL REACTION KINETICS; ETHANE; HYDROXYL RADICALS; METHYL RADICALS; ORGANIC HALOGEN COMPOUNDS; PULSE TECHNIQUES; RADIOLYSIS; RECOMBINATION; SPECTROSCOPY; TROPOSPHERE

UDC 547.412:551.510.534

April 1983
Risø National Laboratory, DK 4000 Roskilde, Denmark

ISBN 87-550-0891-7
ISSN 0418-6435

Risø Repro 1983

FOREWORD

This report presents the results of experimental studies of gas phase elementary reactions between hydroxyl radicals and selected hydrocarbons and halogen substituted hydrocarbons. The work was initiated by a desire to utilize the state-of-the-art pulse-radiolysis instrumentation developed at RISØ in studies of elementary reactions which are known to take place in the atmosphere. The work was supported by a grant from NORDIC COUNCIL OF MINISTERS which allowed us to engage Dr. E. Bjarnov to collaborate with the permanent members of our group during the initial part of the very extensive experimental work.

A progress report (RISØ-M-2337) presented the status of June 1982 based on room temperature experiments conducted by E. Bjarnov. The present final report contains experimental results on a larger series of compounds studied over the temperature range T = 300-400 K. All of the experiments were carried out in one continous sequence during the period July-October 1982. The subsequent analysis of the very numerous experimental data showed that the results on three of the selected compounds had to be abandoned because of small contents of highly reactive impurities present in the applied reactant samples. These compounds (CH_4, CH_3CCl_3 and $CHCl_3$) will be re-investigated in the near future under improved experimental conditions.

TABLE OF CONTENTS

1. SHORT SUMMARY

We have studied a series of elementary reactions between hydroxyl radicals and selected molecular compounds which are released into the troposphere from natural biogenic sources as well as from industrial activities.

The following rate constants and Arrhenius parameters were obtained:

RH	k(OH+RH)	A	E
C_2H_6	2.0×10^8	9.73×10^9	2.33
CH_3Cl	4.3×10^7	1.07×10^9	1.94
CH_2Cl_2	1.0×10^8	4.05×10^9	2.22
$CHFCl_2$	2.9×10^6	1.12×10^9	3.55
CCl_2F_2	$<< 10^6$	no reaction	
	$M^{-1}s^{-1}$	$M^{-1}s^{-1}$	kcal/mol

Hydroxyl radicals were produced by pulse radiolysis of water vapour and the kinetics of OH was followed by kinetic spectroscopy.

The kinetic results of the present investigation were obtained at atmospheric pressure in contrast to previous experimental work where low-pressure techniques have been applied. To calculate tropospheric life times it is of course necessary to find out whether or not the sink reactions with OH radicals exhibit any pressure dependence. We find no evidence for pressure dependence of any of the metathetical reactions above. Much work was devoted to a careful analysis of the effect of CCl_2F_2 on the OH decay kinetics and it was concluded that CCl_2F_2 acts as a very efficient third body for the OH combination reaction. The implications are discussed.

2. Introduction

Pollution has become an important international issue because of a perceived threat to what has become known as the ozone layer, a region of relatively high ozone concentration between 20 and 40 km above Earth's surface. The planet Earth is a cosmic couveuse where the atmosphere serves to protect living organisms against high-energy radiation from outer space and provide an insulating layer maintaining the temperature within the narrow range which is essential for the occurrence of biological processes.

Most of the high-energy radiation is effectively absorbed by the most abundant constituents of the atmosphere, i.e. molecular nitrogen and oxygen. However, ozone plays an important role by absorbing almost completely a biologically harmful part of the solar ultraviolet radiation which is not absorbed by the other atmospheric constituents.

On the basis of general knowledge of chemical reactivity atmospheric scientists realized that two of society's more recent activities could alter the amount of ozone in the stratosphere. One is the use of supersonic jet airplanes cruising through the lower part of the stratosphere. The engines of such aircraft release large amounts of nitrogen oxides that catalytically destroy ozone. The other activity is the use of chlorofluorocarbons (CFCs) in refrigeration systems and in aerosol cans as propellants. As pointed out by Molina and Rowland (1) the chemical inertness and high volatility which make these materials suitable for technological use also mean that they enter

the atmosphere spontaneously upon release and since there are no obvious sinks for their removal in the troposphere (lower 12 km of the atmosphere) the CFCs will ultimately diffuse into the stratosphere.

The CFCs absorb light only in the far ultraviolet region which does not penetrate into the lower part of the atmosphere. However, in the stratosphere light absorption by CFCs gives rise to photochemical release of chlorine atoms followed by an extensive catalytic chain reaction leading to a net destruction of ozone (O_3) and oxygen atoms:

$$Cl + O_3 \rightarrow ClO + O_2$$
$$ClO + O \rightarrow Cl + O_2$$

The potential ozone depletion owing to a continued release of CFCs may have serious consequences on the entire biosphere because of the subsequent enhanced flux of biologically harmful ultraviolet radiation. Since the predictions by Molina and Rowland in 1974 the CFC-problem has entered the public consciousness and the legislative process of many governments around the world.

Consequently, atmospheric scientists have been hard pressed to give confident, or even realistic, predictions about the effect of society's activities on stratospheric ozone.

A Co-ordinating Committee on the Ozone Layer (CCOL) has been established within the United Nations Environment Programme. (UNEP) The aim of the committee is to coordinate the ongoing and planned research programmes relevant to the World Plan of Action on the Ozone Layer. An assessment of ozone depletion and

its impacts is currently updated on the basis of the most recent results accumulated within different fields of atmospheric science, ozone monitoring, chemical kinetics and advanced computer modelling. (2) To set up a realistic model of the atmosphere with the required predictive power is a formidable task due to the overwhelming complexity in chemical kinetics and transport dynamics.

Current computer models incorporate about 140 chemical reactions and at first sight it might seem overoptimistic to expect realistic predictions to emerge from such complex calculations. However, a recent status shows that previous discrepancies between the estimates of models of stratospheric processes and observed concentrations of certain important species have been reduced. (4) One of the most important tasks is of course to establish a reliable data base in terms of experimental rate constants as input for the computer models. Experimental data originating from a fairly large number of active working teams on chemical kinetics are collected and evaluated by the CODATA Task Group on Chemical Kinetics. (3) Another and equally important task is to monitor the concentration profiles of the more important reactive species throughout the atmosphere. This task is accomplished by a large number of groups working with both ground-based and airborne equipment utilizing the most advanced techniques available at present. The success of computer modelling can be tested by comparison with the real world, i.e. the measured concentrations of various species in the atmosphere. These are the hard facts we have to "understand" using the

sophisticated computer models. The computer models may well give "wrong answers" for different reasons. But still the computer models serve as the only possible systematic framework that may eventually allow us to predict the dynamics of the atmosphere, a task that is just within our recent scientific capabilities. One of the key species that plays an important role by controlling the tropospheric life times of many natural and man-made compounds emitted from the Earth is the hydroxyl radical,OH. (3,4) This radical is highly reactive and participates in many combination and atomic transfer reactions. Monitoring of OH in the atmosphere has proved to be a difficult task but recent techniques based on the applications of lasers look very promising. (2) All of the chemical reactions occurring in the atmosphere can in principle be studied in the laboratory thanks to a number of powerful experimental techniques that have been developed within the field of gas phase kinetics. A large amount of experimental work has been devoted to the study of reactions between hydroxyl radicals and halocarbons. (5) Two techniques have been especially favoured in these studies: One is based on discharge flow reactors where the downstream steady-state concentrations of hydroxyl radicals are monitored by resonance fluorescence from the $OH(A^2\Sigma - X^2\Pi)$ transition.

The other technique is flash photolysis combined with either resonance flourescence or resonance absorption detection of OH. The basic idea of both techniques is to study the isolated ele-

mentary reactions of interest, i.e. OH + RH --> H_2O + R without interference from competing reactions. To suppress radical-radical reactions it is required to work with the lowest possible concentrations of OH-radicals. Using resonance fluorescence it is possible to monitor OH-concentrations of 10^9 - 10^{11} cm^{-3}. Under these conditions, the corresponding half-lives of radical-radical reactions are of the order of 0.01 second or longer. For the reaction of interest, OH + RH it is possible to obtain half-lives ($\tau = \ln 2/k(RH)$) that are much shorter than 0.01 sec by proper choice of the halocarbon concentrations (RH). It is essential that this be achieved at moderately low halocarbon concentrations even in the case of "slow reactions", e.g. OH + CHF_2Cl where $k = 4.5 \times 10^{-15}$ cm^3 $molecule^{-1}$ sec^{-1}.

In most cases the experimental results obtained by the two experimental techniques mentioned above are in good agreement. (5) When two different experimental techniques yield essentially the same results it would seem that the rate constants and Arrhenius factors so obtained may be taken with confidence for the given experimental conditions. However, a common feature of both methods is the applied range of pressures which, in general, is much below 1 atm. Thus, it seems that a possible pressure dependence of the various rate constants remains an open question. In view of the "unusual pressure dependence" observed recently in certain OH and HO_2 reactions, it has been realized that measurements of rate constants at higher pressures are very important and require extensive studies.

Discharge flow reactors are typical low-pressure devices and

flash photolysis combined with resonance fluorescence can be used only at moderately low pressures because of fast quenching of the resonant state at higher pressures.

Thus, studies of reaction kinetics at pressures around 1 atm. require other techniques like flash photolysis or pulse radiolysis combined with transient absorption spectrometry.

In the present investigation we apply the technique of pulse radiolysis combined with kinetic spectroscopy to study the reactions between hydroxyl radicals and selected hydrocarbons and halocarbons at a pressure of 1 atm and over a range of temperatures to obtain rate constants and Arrhenius parameters for these reactions.

2. Specific Aims of the Present Investigation:

(I) Experimental determination of rate constants for reactions of hydroxyl radicals with selected hydrocarbons and halocarbons at atmospheric pressure, and over a sufficiently wide range of temperatures to obtain activation energies E_a, as defined in terms of the Arrhenius expression: $k = A \exp(-E_a/RT)$.

(II) Investigation of the capabilities of high dose rate pulse radiolysis combined with transient uv-absorption spectrophotometry in studies of OH reactions in comparison with other known techniques.

Choise of Compounds.

We have chosen methane and ethane as reference compounds because

the rate constants for the reactions $OH + CH_4 \rightarrow H_2O + CH_3$ and $OH + C_2H_6 \rightarrow H_2O + C_2H_5$ are well established at the pressure, and in the range of temperatures of interest. (p = 1 atm, T = 300-400 K) The series CH_3Cl,CH_2Cl_2,$CHCl_3$,CHF_2Cl,CF_2Cl_2 and CH_3CCl_3 was chosen to study the effect of halogen substitution on the rate constant for the reaction with hydroxyl radicals.

While CH_4 and CH_3Cl are present in the troposphere as a result of natural processes in the biosphere the halocarbons CHF_2Cl, CF_2CL_2 and CH CCl are antropogenic, i.e. purely synthetic compounds which are released into the atmosphere by society's activities.

With the exception of CF Cl the tropospheric lifetimes of these compounds are presumed to be controlled by the reaction with hydroxyl radicals which is the only tropospheric sink known at present.

Characteristic Features of the Pulse-Radiolysis Technique.

In many respects, the high dose rate pulse-radiolysis technique applied in the present investigation differs from other techniques that have been used in studies of the reactions between OH radicals and halocarbons.

The most important difference is that competition between simultaneous reactions cannot be neglected nor suppressed in pulse-radiolysis experiments. Thus, the analysis of experimental results obtained by pulse radiolysis requires more sophisticated differential methods to separate out the effect of any selected elementary reaction on the observed overall kinetics which contain contributions from a number of competing reactions. The

applicability of simple analytical procedures was tested against computer models involving the complete set of known competing reactions occurring in the radiolysis of water vapour in the presence of small amounts of additives.

Attempts have been made to identify all possible sources of systematic errors regarding the experimental work as well as computer modelling where a possible neglect of significant reactions may result in erroneous conclusions.

Experimental Background.

Before presenting and discussing the experimental results we summarize the present status of pulse radiolysis of gases, and in particular the radiolysis of water vapour which serves as the source of hydroxyl radicals in the present investigation. Since the timedependent concentration of OH-radicals is monitored by absorption spectrometry we present the most essential features involved in kinetic spectroscopy of OH-radicals.

Finally we explain the experimental strategy and discuss the analytical and computational methods applied in evaluating of the experimental results.

Results and Discussion

A complete documentation of all experimental results is collected in the appendix. The kinetic results for each of eight individual reactants (the selected hydrocarbons and halocarbons) obtained at five different temperatures are presented in tables specifying the applied reactant concentrations and the corresponding kinetic features in terms of half-lives and time derivatives obtained from experimental OH-decay curves.

A master table for each reactant summarizes the variation in rate constant throughout the temperature range, and the corresponding Arrhenius parameters are then derived.

The discussion involves a comparison with the results of previous investigations and an attempt is made to assess the general applicability of pulse radiolysis to studies of atmospheric chemical kinetics.

4. Pulse Radiolysis of Gases.

The technique of pulse radiolysis is one of the most powerful methods for studies of short-lived transient species such as free radicals, radical-ions, and excited states of atoms and molecules.

The technique was developed as a radiation chemical analog of flash photolysis which had been applied very successfully for more than a decade before the advent of electron accelerators which are the sources of pulsed high-energy radiation used in pulse radiolysis. The technique was first applied on liquid systems and later extended to gas-phase studies. An extensive review of pulse radiolysis of gases has been published by Sauer. (6)

In the present investigation we use a field-emission accelerator, Febetron 705 B, as the source of ionizing radiation.

A gas mixture contained in a 1-liter sample cell is irradiated with an intense beam (3000 amp) of 2-MeV electrons with a pulse duration of 30 nsec corresponding to an energy of 180 joule per pulse. The primary effect of the ionizing radiation is production of positive ions and secondary electrons (which may in turn cause further ionization) and excited atoms and molecules. Neutral

fragments, i.e. atoms and free radicals are formed as a result of very fast ion-neutralization reactions and decomposition of excited states. The "stopping power" of gases at a pressure of 1 atm is very low for 2-MeV electrons. Only a small fraction of the total energy is absorbed while the electrons pass through 10 cm of a gas at 1 atm.

However, with the Febetron 705 B we can produce free radicals in concentrations of about 10^{-6} moles/liter and in most cases this is sufficient for detection by fast optical absorption spectrometry. The low stopping power for 2-MeV electrons ensures a fairly homogeneous energy deposition and radical production throughout the gas sample. The energy absorbed by the gas causes ionization and excitation of at most one in 10^5 molecules and the overall change in temperature due to the primary energy deposition, and including the heat of chemical reactions amounts to a maximum of one or two degrees; such a small change can generally be ignored with respect to its effect on reaction rates. Thus, the disturbing concentration gradients and local heating, which are problems frequently encountered in flash photolysis experiments, are largely avoided by the pulse-radiolysis technique. Another advantage of the high dose rate pulse-radiolysis technique is that the observed half-lives of the transient species are normally much shorter than the time required for diffusion to the walls of the reaction vessel. Hence, in pulse-radiolysis experiments we also avoid "wall effects" which remain a serious problem in low-pressure discharge flow reactors which are wi-

dely used for studies of free-radical gas phase kinetics. While in some respects pulse radiolysis for the reasons summarized above may be considered superior to other gas kinetic techniques, it should be pointed out that the interpretation of experimental kinetic data obtained by pulse radiolysis may often be difficult due to the inherent complexity of the reaction mixture.

These problems arise because of the simultaneous production of different transient species which may all react with each other. The simultaneous production of different transient species is unavoidable in all but the simplest diatomic systems like H_2, where the only possible "radical species" is the H-atom. For a simple triatomic system like water there are three possible neutral fragments, H,O and OH and it wil be necessary to take into account all of the possible combination reactions. At first sight it may seem that too many things happen at the same time so that a complete analysis would be a hopeless task.

However, as will be shown in Part 7, rather simple procedures may be used to analyze the effect of an additive reacting with only one of the primary radicals, e.g. the hydroxyl radical. The variation in half-life with increasing concentration of the additive follows a simple analytical expression which may be used to calculate the value of the rate constant k(OH+ Additive). A more rigorous method utilizes the shape of the entire decay curve which becomes exponential in the limit of sufficiently high concentrations of additive. The use of

computer models to simulate the reaction kinetics is the most powerful tool available in analysing experimental data, in particular when dealing with more complex cases. Also, the response of the model to changes in experimental parameters like irradiation dose and chemical composition may help in defining optimum experimental conditions where the effect of a particular elementary reaction may be enhanced. Finally, the computer simulations may be used as a critical test of a proposed model in comparison with the experimental results.

5. Radiolysis of Water Vapour

The radiolysis of water vapour has been studied extensively by the use of steady-state as well as pulse-radiolysis techniques. An excellent review is given by Dixon. (7)

Pulse radiolysis of water vapour is a very useful method for the production and kinetic studies of hydroxyl radicals. Gordon and Mulac have studied metathetical reactions of OH with a number of polyatomic molecules. (8) Most of the experiments were carried out at elevated temperatures in order to obtain high enough partial pressures of water. The OH decay curves were recorded by monitoring the characteristic transient UV absorption. In pure water vapour at partial pressures above 65 torr the OH radicals decayed by second-order kinetics. Based on a calculated initial yield of OH radicals Gordon and Mulac determined the value of $2k(OH+OH) + k(H+OH) = 2 \times 10^{10}\ M^{-1}s^{-1}$.

Boyd, Willis and Miller have investigated the radiolysis of water vapour at very high dose rates. (9) Based on studies of

the effect of H-atom scavengers (HBr and HCl) on the yield of molecular hydrogen they determined the yields of the neutral transient species, G(H) = 7.45, G(OH) = 6.25, and G(O) = 1.05 per 100 eV of absorbed energy. In the presence of an electron scavenger (SF_6) the yield was reduced to G(H) = 4.15. As this difference, $\Delta G(H) = 3.3$ is the same as the known ion-pair yield in water vapour it was concluded that the positive ions formed initially (H_2O^+ and OH^+) end up as hydrated proton clusters which in pure water are neutralized by capture of secondary electrons to form H-atoms. In the presence of SF_6 however, no H-atoms are formed by ion-neutralization. Proton transfer to SF_6^- to form HF and SF_5 was suggested.
A computer model was used to simulate all of the atomic and radical reactions involved in the radiolysis of water vapour and unknown rate constant ratios were adjusted to obtain the best possible agreement with the experimental yields.
Since this model accounts properly for the observed experimental yields it seems that the "tuned values" of the relative rate constants may be taken with confidence. Absolute values of the rate constants were derived using $2k(OH+OH) + k(H+OH) = 2 \times 10^{10}$ $M^{-1}s^{-1}$ as determined by Gordon and Mulac.(8)
Thus, the basis for a quantitative description of the radiolysis of pure water vapour and water vapour with small amounts of radical scavengers present has been established and proved successful. The computer model applied in the present investigation is essentially the same as the one proposed by Boyd, Willis, and Miller. However, in some of our experiments around

room temperature where the partial pressure of water is fairly low we had to take into account the effect of third bodies on the rate of radical combination reactions, e.g. OH + OH + M --> H_2O_2 + M where M symbolizes the contribution from all of the species present, M = Ar, H_2O, etc. In addition, at the lower temperatures we back up with Ar to a total pressure of 1 atm. to maintain the "stopping power" which is approximately proportional to the density of the gas mixture. This also implies "Ar-senthisized radiolysis" where the radicals are formed primarily by energy transfer Ar^* + H_2O --> Ar + H + OH rather than by direct ionization. Consequently we also expect that the relative yields of H,OH and O may differ from the values quoted by Boyd et al.

6. Kinetic Spectroscopy of Hydroxyl Radicals.

The ultraviolet absorption spectrum of OH is well known and the complex structure has been analysed to provide an unambiguous assignment of vibrational and rotational quantum numbers for all of the individual states participating in the $X^2\Pi$ -> $A^2\Sigma^+$ transition. An excellent summary of fundamental data is given by Dieke and Crosswhite. (10) A more elaborate analysis of essentially the same data has been accomplished, based on a computer program employing statistical methods, on the complete set of spectral lines simultaneously to obtain improved spectroscopic constants for the $X^2\Pi_i$ ground state and the $A^2\Sigma^+$ excited state of OH. (11)

6.1 Emission Spectrum.

It is fairly easy to obtain an emission spectrum of OH-radicals showing some of the characteristic rotational levels even with a spectrograph with a moderate resolving power.
A part of the 0,0 band of the OH($A^2\Sigma^+ \rightarrow X^2\Pi$) emission spectrum is shown in Fig.1
The spectrum was produced by maintaining a 2450-MHz microwave discharge through a stream of argon saturated with water vapour at 25 ^oC flowing through the resonator at a rate of 2 ml/min and pressure of 1 torr. The spectrum was recorded with our Hilger and Watts monochromator using a scan rate of 10 Å/min. The focal length is 100 cm, and with a 1200 l/mm grating blazed at 3000 Å; the reciprocal dispersion is 8 Å/mm. A slit width of 0.05 mm was chosen corresponding to a spectral band pass of 0.4 Å. Thus, 0.4 Å is the apparent width of any single line appearing in the spectrum and lines lying less than about 0.5 Å apart will, of course, be unresolved. In Fig.1 some of the indicated members of the Q_1-branch appear well separated while the strong and broad feature at about 3090 A clearly contains a number of unresolved lines. (Q_17 as well as three members of the Q_2-branch)

6.2 Absorption Spectroscopy

A quantitative measure of the light absorption by a pure substance is given by the "LAMBERT-BEER LAW":

(I) $A = \log(I_o/I) = \varepsilon LC$

where A is the absorbance defined in terms of the intensities of the incident (I_o) and transmitted (I) light beam after traver-

sing an optical path length of L cm through the absorbing substance present with a concentration of C moles/liter. The "extinction coefficient" ε in (liter/mole x cm) is a constant characterizing the maximum absorption of the particular substance. The relation holds strictly for "monochromatic light" at the wave length of the absorption maximum. In practical terms an analysing light beam may be considered "monochromatic" after passing a spectrographic device with a spectral band pass which is about 1/10 of the "line width" of the spectral feature under investigation. If this condition is unfulfilled the measured absorbance will be a nonlinear function of C and L and expression (I) will have to be replaced by an experimentally derived function, A = A(C,L). This is the situation that we are facing in the actual case of OH-radical absorption spectroscopy with a medium-resolution spectrograph. The first successful attempts to utilize the ultraviolet absorption spectrum to monitor transient OH-concentrations were carried out as early as 1938-39 by Kondratjew (12) and by Oldenberg and Rieke. (13a)

Using a Fabry-Perot interferometer with a resolving power of 5×10^5 in a tandem combination with a Hilger E1 spectrograph (5.2 Å/mm) Oldenberg and Rieke (13b) was able to measure the absorbance at the line center of $Q_1(6)$ using a spectral band pass of about half the calculated Doppler line width at 300 ^{o}K. (0.01 Å). Using a known concentration of OH-radicals of 1.1×10^{14} cm^{-3} they measured an absorbance of $A = \log(I_o/I) = 0.143$ with an optical path length of L = 150 cm. The corre-

sponding molar decadic extinction coefficient may then be calculated:

$\varepsilon_{Q} = 5.2 \times 10^{3}$ liter/mole x cm

for the line-center of $Q_1(6)$.

Oldenberg and Rieke used these figures to evaluate the absolute thermolecular rate constant for the reaction OH + H + M -> H_2O + M based on relative kinetic measurements obtained previously. (13)

6.3 "Modified Beer's Law Expression"

A modified expression has been proposed (14,15,16):

(II) $A = (\varepsilon LC)^n$

where the fractional power, n is an empirical constant that must be determined experimentally by studying the functional dependence A = A(C,L) under spectroscopically well-defined conditions. Expression (II) was found to be a useful approximation within a limited range of absorbance.

6.4 Determination of Beer's Law Exponent, n

Defining

LW = true line width of the spectral feature in Å

BP = spectral band pass = SxD

S = slit width in mm

D = reciprocal dispersion in Å/mm

we find that n < 1 when BP > LW

and n -> 1 when BP/LW -> 0

Since the calculated Doppler line width LW = 0.01 Å at 300°K for the individual rotational lines of OH, and the dispersion-

limited minimum band pass of our Hilger and Watts spectrograph is BP = 0.08 Å, we expect to find n-values, n<<1 for measurements on isolated rotational lines. However, instead of selecting an isolated rotational line for transient absorption measurements we find that a larger absorption signal may be obtained by tuning the center of the spectral band pass to a "crowded region" where several close-lying lines may be collected within the band pass.

In our measurements of transient absorption signals the analysing light source is a 150-W high-pressure Xe-lamp which emits a broad continuum from about 1900 Å to 9000 Å and with a maximum around 4000 Å. A pulsing device with optical feedback provides a fiftyfold enhancement of the light intensity in the UV-region.

In terms of light intensity per spectral band pass this lamp was found superior to a microwave-powered OH-resonance lamp which did not provide an acceptable signal-to-noise ratio in the short time scales required in the present studies of fast OH-kinetics. The light intensity monitored by the photomultiplier is proportional to the spectral band pass, i.e. with the chosen width of the entrance and exit slits. An acceptable S/N ratio can be obtained only if a sufficient number of photons hit the photocathode during the characteristic half-life of the transient, which in the case of OH has a maximum value of about 100 μsec under our standard experimental conditions. To obtain S/N = 100 in experiments covering half-lives of 1-100 μsec we had to use a slit width S = 0.1 mm

corresponding to a spectral band pass of BP = 0.8 Å.

6.5 "Best Compromise"

As a best compromise between spectral resolution and S/N ratio we have chosen to monitor the transient OH-absorption using the 3090 Å feature shown in Fig.1 and a band pass BP = 0.8 Å. Under these conditions we obtain a S/N ratio of about 100 corresponding to a maximum absorbance of AMAX = 0.150 observed at the end of the radical-generating 2-MeV electron pulse. Experimental values of the "Beer's Law Exponent" were found to vary within a range of $n = 0.73 \pm 0.10$.
Since plots of log(A) versus L and C were found to be nicely linear within the range of interest (A = 0-0.150) we assume that the "true value" of the concentration of OH-radicals is well approximated by $(OH) = (OH)_o \times (A/AMAX)^{1/0.73}$.
Experimental details are given in Appendix 1.

7. Analysis of Complex OH-Radical Kinetics

The experimental results are obtained by kinetic spectroscopy of hydroxyl radicals (OH) formed by irradiating water vapour plus small amounts of additives with a short pulse (4×10^{-8} s) of high-energy electrons (2 MeV). The effect of the irradiation is to dissociate water molecules into H-atoms and OH-radicals:

$$H_2O \text{ - - -> } H + OH$$

In the absence of additives the fate of H and OH is governed mainly by the reactions:

(1) $OH + OH \rightarrow H_2O_2$

(2) $H + OH \rightarrow H_2O$

(3) $H + H \rightarrow H_2$

Consecutive reactions of H and OH with accumulating product molecules H_2 and H_2O_2, play only a minor role in single-pulse high-dose rate experiments.

Under these conditions the decay of OH and H is to a good approximation described by the differential equations:

(I) $-d(OH)/dt = 2k_1(OH)^2 + k_2(H)(OH)$

(II) $-d(H)/dt = 2k_3(H)^2 + k_2(H)(OH)$

The decay of hydroxyl radicals can be studied by monitoring the transient absorbance of one of the characteristic rotational lines of the $OH(A^2\Sigma^+-X^2\Pi)$ rovibronic transition in the region 3000 - 3200 Å. The observed transient absorbance is a direct measure of the concentration of hydroxyl radicals at any given time during the decay.

Figure 1 shows an example of the transient absorbance of OH monitored at 3089.6 Å in the absence of additives. The absorbance decreases to half of the maximum value in the course of 100 µsec and this "natural half-life" must be ascribed to the combined rates of reactions (1) and (2). Another characteristic feature is the long "second-order tail" following the steep initial part of the decay.

The high reactivity of OH-radicals observed in many H-abstraction reactions,

(4) $R\text{-}H + OH \rightarrow R + H\text{-}OH$

is due to the high bond energy, D(H-OH) = 118 kcal/mole, which exceeds the bond energies D(R-H) of most other hydrides, such as simple hydrocarbons (CH_4,C_2H_6,C_3H_8,etc.), and substituted hydrocarbons like methyl chloride and chloroform. In general, the observed rate constants are higher the higher the difference in bond energies, D(H-OH) - D(R-H).

Addition of a "substrate", RH reacting in accordance with (4) has a characteristic effect on the observed decay of OH, as shown in Fig.2. Comparison with Fig.1 reveals a substantial suppression of the "second-order tail" and also that the half-life is reduced relative to the "natural decay".

In the presence of RH an additional term must be added to (I),

$$\text{(III)} \quad -d(OH)/dt = 2k_1(OH)^2 + k_2(H)(OH) + k_4(RH)(OH)$$

This differential equation serves as the basis for our determinations of the rate constants k_4 for the elementary reaction between OH-radicals and selected substrate molecules, RH.

The simultaneous occurrence of (1),(2),(3) and (4) of course presents a complication in the sense that one has to make proper corrections for the contributions from (1),(2) and (3) to the observed overall decay rate. In general, this can be accomplished by studying the effect of reaction (4) over a sufficiently large range of substrate concentrations. In the limit of very high RH-concentrations, (i.e. when $k_4(RH) >> 2k_1(OH)$ and $k_4(RH) >> k_2(H)$) the differential equation (III) degenerates into

$$\text{(III*)} \quad -d(OH)/dt = k_4(RH)(OH)$$

corresponding to a simple exponential decay

$(OH) = (OH)_o \exp(-k_4(RH)_o t)$

with a characteristic half-life

$\tau = \ln 2/k_4(RH)_o$.

This expression may be used to obtain a quick estimate of the value of k_4 from a single experiment in which the RH-concentration was high enough to push the observed half-life down to a small fraction of the "natural half-life".
Problems arise in studies of "slow reactions" where it may be difficult to fulfill the requirement $k_4(RH)_o >> 2k_1(OH)_o$.
Based on computer simulations we find that it is still possible to calculate a reliable value of k_4 based on a relatively small variation in half-lives by applying the equation

(IV) $\quad 1/\tau = 1/\tau_o + \ln 2/k_4(RH)_o$.

According to this equation a plot of reciprocal half-lives versus the corresponding RH-concentrations is a linear function with a slope equal to $\ln 2/k_4$.
This is a simple method which allows a quick determination of the rate constant k_4 based solely on measured half-lives and the corresponding substrate concentrations. It must be kept in mind, however, that the method is based on the assumption that the kinetics degenerates into a pseudo-first-order exponential decay (III*) at sufficiently high substrate concentrations.
Our experiences with F12 (CF_2Cl_2) as the substrate provides an

interesting example where the observed decrease in half-lives with increasing F12-concentrations must be assigned to an entirely different reaction mechanism. This becomes clearly evident by inspection of the complete decay curves which remain typically second order (long tail) although the half-lives do decrease with increasing substrate concentrations.

A more rigorous procedure which allows a clear distinction between first- and second-order kinetics is to analyze plots of lnA versus time, where A is the transient OH-absorbance. Such a plot becomes strictly linear when the decay degenerates into pseudofirst-order kinetics at high substrate concentrations in accordance with (III). Any significant contributions from reactions of OH with itself or other short-lived radicals will show up in terms of a more-or-less pronounced curvature. Thus, if a particular curve is found to be linear (within the experimental noise) it means that the decay is almost completely controlled by the last term in Equation (III) and hence, the slope $d\ln A/dt = k_4(RH)_o$ + CORR, where "CORR" is a small correction term due to contributions from the radical-radical reactions. The magnitude of the correction term is related to the curvature which may be hard to detect due to the experimental noise level. We subtract the correction term by "double differentiation" of a series of decay curves corresponding to different substrate concentrations:

$$(V) \qquad k_4 = d(d\ln A/dt)/d(RH)$$

We have applied both methods (IV) and (V) and we find that the

calculated values of k_4, using either method, are the same within the experimental uncertainties. We expect of course the values calculated via (IV) to exhibit a larger scatter than those based on (V) because the former utilizes only a single point of the curve (half-life) while the latter involves all points on the decay curve.

The simple mathematical procedures outlined above have been tested against ideal noise-free decay curves produced by computer simulations of reactions (1) through (4). Such idealized curves (without contamination by the unavoidable noise observed on all experimental curves) are very instructive as a basis for the evaluation of the experimental data. The complete absence of noise makes it possible to study the exact shape of the decay curves including the curvature of (lnA versus t)-plots which decreases rapidly from a maximum value at (RH) = 0 to a very small value at moderate RH-concentrations where the half-life of OH is reduced by only a factor of 2-3. Thus, the model curves are very helpful in defining "normal behavior" and "what to expect".

8. Gas Phase Pulse Radiolysis Instrumentation.

The experimental set-up is shown in Figure 1. The field emission accelerator (FEBETRON 705B) provides single pulses of 2-MeV electrons with a pulse duration of 30 nsec and a maximum current of 3000 amperes.

The gas samples are contained in a stainless steel irradiation cell mounted directly onto the accelerator. We are most grateful to Gordon and Mulac from Argonne National Laboratory for kind permission to copy the cell design which they developed during their pioneering work on high dose rate gas phase radiolysis. (16)

The optical arrangement involving an internal set of conjugate mirrors was first described by White. (17) By this device the optical path length may be increased by multiple passages of the analyzing light beam through the gas sample. Most of the experiments were carried out using twelve traversals corresponding to an optical path length of 120 cm.

Gas mixtures were prepared by admitting one component at a time and reading the corresponding partial pressure using a MKS Baratron model 170 absolute electronic membrane manometer with a resolution of 10^{-5} Bar.

Electric heating and temperature control provides a range of sample temperatures from 300 to 400° K. A platinum-resistance thermometer is used to measure the temperature of the gas mixture near the central part of the irradiation cell traversed by the analyzing light beam. The principal features of the optical system is shown in Fig. 2.

The analyzing light source is a 150-watt high-pressure xenon lamp with short axial arc and parabolic reflector. The sapphire exit window transmits the Xe-continuum down to about 1900 A. An optical train of suprasil lenses and front-surface aluminized mirrors carries the analyzing light through the sample cell to the entrance slit of the Hilger and Watts MONOSPEK 1000 monochromator. A great effort has been made to obtain a high throughput in the ultraviolet region and to reduce the amount of stray light entering the monochromator.

The weakly divergent light beam from the xenon lamp is focused onto a discriminating slit plane to form an image of the high-level xenon arc. This slit is essential to the performance of the entire optical system. The slit selects only that fraction of the light which can be transmitted through the monochromator entrance slit and fill out the full aperture while the major part of the light, which can contribute to only unwanted scattered light and photolysis, is rejected. Due to the dispersion (refractive index versus wavelength) the first suprasil lens combined with the slit acts as a band-pass filter which transmits the light in only a particular wavelength range determined by the distance between the lens and the slit plane. This feature is found to be important also for the optical feedback to the xenon lamp pulser which receives a spectral representative light signal via the quartz plate beam splitter and fiber optic cable. The xenon lamp pulser is most essential to the performance in the ultraviolet region where the light intensity is increased by a factor of 20-50 in light

pulses stabilized to within a few per cent and with a duration of several milliseconds.

The shape of the transmitted light beam is shown in a plane orthogonal to the longitudinal direction of the first discriminating slit which is parallel to the entrance slit of the monochromator.

For a given wavelength the distance between the telescope lens pair and the neighbouring lenses is chosen so that a circular image of the limiting aperture fills out the collecting monochromator mirror for maximum light efficiency.

The application of a total of seven lenses implies a large loss of light intensity (about 4-6% per surface) which makes the use of the lamp pulser indispensable. However, a major advantage of the system is that the lenses act as a premonochromator resulting in a very low level of stray light which amounts to a maximum of only a few percent at 2000 Å.

The analyzing light is dispersed in the Hilger and Watts monochromator which has a focal length of 100 cm and an aperture ratio of 1/10. For the ultraviolet region we apply a ruled grating with 1200 grooves/mm and blazed at 3000 Å. The reciprocal dispersion in the plane of the exit slit is 8 Å/mm.

The light intensity over the wavelength band-pass selected by the exit slit is monitored using a Hamamatsu R 955 photomultiplier coupled to a current input operational amplifier with adjustable offset. The transient signals are stored in a Biomation 8100 wave form digitizer interfaced to a PDP8 minicomputer. Plots of transient absortion versus time, as well as simple

first- and second-order kinetic plots are immediately available on a display screen and may be displayed on an X-Y recorder or stored on magnetic tape for further processing on a large central computer system.

Dosimetry was performed by monitoring the optical absorbance of ozone formed by irradiation of 1 atm of oxygen. Using $G(O_3)$ = 12.8 (18) and $\epsilon(O_3)$ = 3067 $M^{-1}cm^{-1}$ at 2550 Å (19) we calculate a dose of 125 krad per irradiation pulse.

9. Computer Facilities

Computers have become important tools in experimental chemistry. In the present investigation we utilize a PDP8 minicomputer for compilation and edition of experimental data files which are transferred to a Burroughs 7800 central computer for further data processing and analysis.

The on-line minicomputer is used to collect the experimental kinetic curves which are temporarily stored in a fast waveform digitizer. Each transient curve is composed by 2000 time-equidistant samples of the transmitted light intensity in 8-bit representation corresponding to a resolution of 1/256. The minimum time increment between samples is 10 nsec. Comment lines specifying the experimental conditions are attached to each individual kinetic curve during the build-up of the raw data file. Algorithms are available to convert the raw data into absorption versus time curves or other relevant representations which can be displayed to inspect the data quality before plotting or transferring to magnetic tape.

The magnetic tapes are brought to a large central computer where the experimental data become available as disk files with access from special programs which are used for analysis of the reaction kinetics. The signal-to-noise ratio of the experimental raw data may be improved, if necessary, by averaging repetitive runs or by applying smoothing procedures. Analytical first- and second-order decay curves may be fitted to the experimental curves by least-square procedures to obtain a significance test of the reaction order and standard deviation of the corresponding rate constant. Complex kinetics involving a mixture of first- and second-order components are frequently encountered and in these cases it is often possible tc resolve the individual contributions by studying the shape of log(concentration) versus time curves which are linear in the first-order limit (tail-end) and strongly curved in the initial part of the decay if a second-order component is significant. In general, the analysis involves a study of the functional dependence of the shape of the decay curves following a change in the concentration of one of the reactants. The characteristic feature may be either the reciprocal half-life or a time derivative. The observed variation in the case of "forced competition" is, in general, a simple linear function of the reactant concentration, as described in Part 7. Our most powerful computational tool is simulation of the complete set of chemical reactions involved. We use a program developed by O. Lang Rasmussen (20). As input, this program accepts reaction schemes in the usual chemical notation, e.g., H + OH

-> H_2O, $k=2x10^{10}$, etc. The program translates the "chemical equations" into the pertinent set of differential equations which is solved by numerical integration after specification of initial concentrations, irradiation dose, etc. Computer simulations are conducted much faster than real experiments and the effect of parameter variation on the model kinetics can be studied very quickly using a graphical computer terminal. In this way we have been able to find out in which cases it is safe to apply simple analytical procedures to calculate rate constants from the experimental decay curves.
Computer simulation is also an indispensable tool in the analysis of "odd cases" like the CFC-12 case, as described later.

10. Results and discussion

The experimental results comprise spectro-kinetic studies of hydroxyl radicals reacting with selected hydrocarbons and halogenated hydrocarbons under varying experimental conditions. For each of the selected reactants the decay of OH was studied at five different temperatures, and at each temperature over a range of reactant concentration.
The selected reactants are

Methane family

CH_4, CH_3Cl, CH_2CL_2, $CHCl_3$, CHF_2Cl and CF_2Cl_2

Ethane family

C_2H_6 and CH_3CCl_3

The experimental data base amounts to about 500 individual OH decay curves which were analyzed by the procedures discussed in part 7.

We present rather detailed discussions of two extreme cases:

Simple standard case: $OH + C_2H_6 \rightarrow H_2O + C_2H_5$

This is a fast reaction, the kinetic analysis is simple and the results are unambiguous.

Complex case: $OH + CF_2Cl_2 \rightarrow ?$

CFC-12 is expected to be completely inert toward attack by OH radicals.

Much to our surprise the half-life of OH decreased upon addition of CFC-12. The complex non-exponential decay was analyzed by comparison with different computer models.

We then proceed with a shorter discussion of the other reactant molecules.

10.1 $OH + C_2H_6 \rightarrow H_2O + C_2H_5$

The reaction kinetics was studied by monitoring the transient $OH(X^2\Pi \rightarrow A^2\Sigma)$ absorption at 3090 Å.

A summary of the experimental conditions is given in the table:

t	$P(H_2O)$	$P(C_2H_6)$	No. of exp.
27	20	0 - 3.5 - 7.2 - 10.4	8
49	50	0 - 1.1 - 2.1 - 5.0 - 10.0	18
97	100	0 - 2.3 - 5.3 - 11.0	12
127	200	0 - 2.7 - 5.0 - 9.6	11
°C	mbar	mbar	49

At each temperature the partial pressure of water was kept constant while the partial pressure of ethane was varied to promote the "forced competition" between the title reaction and the "natural decay channels" for OH.

The gas mixtures were prepared by admitting one component at a time to the sample cell which was carefully evacuated before the filling.

A high-performance membrane manometer (MKS BARATRON, 170 series) with a linear dynamic range of 1 - 10^{-5} atm was used to obtain accurate values of the individual partial pressures.

In all experiments the total pressure was kept at 1 atm by backing up with high-purity argon. The temperature of the gas mixture was measured with a calibrated platinum resistance thermometer with a probable error limit of $\pm 1^0$ C.

In principle the rate constant for the title reaction is calculated from the response of a characteristic kinetic feature (e.g. half-life) to the change in the concentration of ethane. As discussed in Part 7, the simple relation $\tau = \ln 2/k(C_2H_6)$ holds in the limit of high concentrations. Thus, all we need in order to calculate the rate constant is the measured half-life (τ) and the corresponding concentration of ethane.

The half-life is a simple and well-defined quantity which can often be measured very accurately.

However, to calculate the ethane concentration, $(C_2H_6) = p/RT$ we need accurate readings of the partial pressure (p) and the temperature. While these measurements are straightforward at room temperature problems arise when "cold" gases are admitted

to the heated sample cell. After admission of C_2H_6 at elevated temperatures we observed a slow rise in the reading of the partial pressure and we ascribe this "relaxation" ascribe to equilibration of the temperature through gas-wall collisions. Thus the reading of the "true pressure" corresponding to the chosen temperature required a rather ill-defined time delay to obtain the limiting stationary pressure. We frequently checked the leak-rate into the evacuated cell in order to estimate the possible interference with the reading of $p(C_2H_6)$. We estimate a probable overall error limit of $\delta p(C_2H_6) = \pm 0.5$ mbar at 127°C while at 27°C it is a factor of five lower, $\delta p(C_2H_6) = \pm 0.1$ mbar.

Combining the uncertainties in the measurements of temperature and partial pressures we get an estimate of the error limits for the calculated concentrations of $\delta C = \pm 4 \times 10^{-6}$ moles/liter at 27°C and $\delta C = \pm 2 \times 10^{-5}$ moles/liter at 127°C.

So far we have considered only the static parameters $(T, (C_2H_6))$ which can be adjusted within the stated error limits in our studies of the competition between the title reaction and the natural OH decay channels. We now turn our attention to the kinetic features.

For the analysis of experimental decay curves we have developed an interactive computer program utilizing a graphical terminal. Individual experimental decay curves are called from the storage of a large central computer by specifying the name of a resident data file and the run numbers. Each experimental

curve is accompanied by file identification and specification of the experimental conditions. Figure 1 in Appendix A10 shows a hard copy of a series of curves as displayed on the graphical terminal.

The program provides the following options:

(1) Standard plot of $(A/A_{max})^{1/n}$ versus time (t), where A is the transient absorption and n the Lambert-Beer modifier as defined in Part 6.3. The program traces the curve and prints out values of A_{max}, t(1/2) and t(1/4), i.e. the maximum absorption and the half-life and quarter-life of the decay. Averaging of several curves and/or digital smoothing procedures may be applied to improve the signal-to-noise ratio.

(2) Logarithmic plot: $\log(A/A_{max})$ versus time, and print out of the slope dlnA/dt obtained by a least-square fitting procedure.

(3) Co-plot of experimental curves and simple model curves. If $t(1/4) < 2.2\ t(1/2)$ the program assumes first-order kinetics and plots $C/C_o = \exp(-k^*t)$ using $k^* = \ln 2/t(1/2)$. Otherwise, if $t(1/4) > t(1/2)$ the program draws an analytical second-order curve $C/C_o = 1/(1+2kC_ot)$.

These options are normally sufficient for the analysis of simple decay curves by displaying the significant features of first- and second-order reaction kinetics.

In Fig.1 the upper left curve shows the transient OH absorption produced by pulse radiolysis of a gas mixture composed of 200 mbar of water vapour and backed up with argon to 1 atm at 127°C.

The horizontal axis spans a time scale of $0-10^{-3}$ seconds while the vertical axis represents the transient OH absorption monitored at 3090 Å using an optical path length of 120 cm. A spectral band pass of 0.8 Å. n=0.69 was used in the standard plot of $(A/A_{max})^{1/n}$. The absorption builds up to a maximum A_{max} = 0.126 within a few microseconds after the irradiation pulse which has a duration of only 30 nanoseconds. The decay proceeds with a half-life of about 82 microseconds and a typical second-order tail characteristic to the "natural decay channels", OH+OH->H_2O_2 and H+OH->H_2O.

The smooth curve superimposed on the noisy experimental curve is drawn in accordance with the simple second-order expression, $C/C_o = 1/(1+2kC_ot)$ using $2kC_o = 2/(t(1/4)-t(1/2))$ and locked to the points corresponding to $A=0.5A_{max}$ and $A=0.25A_{max}$ on the experimental curve. The fit is quite good particularly at the tail-end of the decay. Likewise, the logarithmic plot shown to the right is nonlinear in accordance with second-order kinetics.

For a genuine second-order reaction $t(1/2) = 1/2kC_o$ and also $t(1/4) = 3 \times t(1/2)$. Since the tail-end is the most characteristic feature of a second-order reaction we apply $2kC_o = 2/(t(1/4)-t(1/2))$ as the "best value" of the experimental half-life. This choice ensures that the tail-end is well accounted for.

The lower left curve shows the OH decay in a gas mixture containing 2.7 mbar C_2H_6 plus 200 mbar H_2O and backed-up with argon to 1 atm. The time scale is now reduced to 0-200

microseconds. In comparison with the upper curve the "second-order tail" is now completely suppressed and the experimental half-life is much shorter, t(1/2) = 15.8 usec.
Clearly, in the presence of 2.7 mbar C_2H_6 the decay has changed into pseudofirst-order kinetics as evidenced by the linear logarithmic plot shown to the right and by the smooth exponential curve to the left which fits the experimental decay curve within the noise. Thus, the decay rate is primarily controlled by the title reaction when $(C_2H_6) = p/RT = 8.23 \times 10^{-5}$ moles/liter. (p=2.7 mbar,T=400 K) As discussed in Part 7 we make use of two simple expressions to calculate the rate constant:

(I) $\quad 1/\tau = 1/\ \tau_o + k(C_2H_6)/\ln 2$

(II) $\quad d(\ln A)/dt = I_o + k(C_2H_6)$

where τ is used as a short notation for the half-life, t(1/2) and index o refers to the "natural decay" in the absence of C_2H_6. While the intercept in (I) is welldefined in terms of the natural half-life τ_o it is not obvious how to assign a value to the constant I_o appearing in expression (II). The problem is that the the log-plot is nonlinear for the natural second-order decay so that d(lnA)/dt is not a constant.
The difficulties regarding the intercept in expression (II) may be bypassed by studying the effect of increasing $p(C_2H_6)$ and applying "double differentiation" to calculate the value of the rate constant, $k = d(d(\ln A)/dt)/d(C_2H_6)$.
In Fig.2 of A10 we show the results obtained at higher partial

pressures of ethane. With $p(C_2H_6)$ = 5.0 mbar (upper left curve) the computer finds an experimental half-life of 9.4 microseconds. The smooth exponential curve $C/C_o = \exp(-k^*t)$ starting at the maximum of the experimental curve and with $k^* = \ln 2/(9.4 \times 10^{-6})$ actually crosses the experimental curve and has a slightly higher tail-end. This effect is even more pronounced with the lower left curves where $p(C_2H_6)$ = 9.6 mbar. The reason for the curve crossing is that the formation of OH via ion-neutralization and other reactions proceeds with a half-life that is not negligible compared with the decay half-life. Therefore, both source and sink terms contribute to the curve shape around the absorption maximum and the experimental half-life is somewhat longer than that corresponding to the title reaction. However, the tail-end of the decay is practically free of interference from the short-lived source terms. Thus, while $t(1/4) = 2 \times t(1/2)$ for a genuine first-order reaction, we find in general $t(1/4) < 2 \times t(1/2)$ for all experimental decay curves in the presence of C_2H_6. To avoid systematic errors due to the build-up terms we substitute $\tau = t(1/4)-t(1/2)$ when using expression (I). This perfectly legal "trick" should work provided that the "induction period", where the source terms are active, is shorter than the decay half-life.

The method based on expression (II) seems to be more reliable because it takes into account the entire experimental curve and allows a clear distinction to be made between first- and second-order kinetics. The log-plots shown to the right in

Fig.2 are linear in accordance with (II) and the slopes can be determined to within an estimated error limit of ± 5%.
Below we summarize the experimental results obtained at 127°C. The values of t(1/2), t(1/4) and dln(OH)/dt are those printed out below the experimental curves in Figs. 1 and 2.

(C_2H_6)	t(1/2)	1(1/4)	$1/\tau$	dln(OH)/dt
0	81.5	216	1.5×10^4	0.76×10^4
8.24×10^{-5}	15.8	29.5	7.3×10^4	4.37×10^4
1.53×10^{-4}	9.1	16.8	1.3×10^5	8.37×10^4
2.93×10^{-4}	6.1	10.2	2.4×10^5	1.60×10^5
moles/liter	μsec	μsec	s^{-1}	s^{-1}

Note: $\tau = t(1/4)-t(1/2)$ was used when $(C_2H_6)>0$.

In Fig. 3 of A10 we plotted the experimental results in accordance with expressions (I) and (II), respectively. From the slopes we obtain:

$k(I) = 5.3 \times 10^8\ M^{-1}s^{-1}$ and $k(II) = 5.4 \times 10^8\ M^{-1}s^{-1}$

Values of τ and dln(OH)/dt were reproducible within ± 5% in repetitive experiments. Regarding the concentration of ethane we estimated an error limit of $\delta(C_2H_6) = \pm 2 \times 10^{-5}$ moles/liter. Combining these uncertainties we find

$$k(OH+C_2H_6) = (5.4 \pm 0.2) \times 10^8\ M^{-1}s^{-1} \quad \text{at } 127^oC$$

The error limit of about ± 5% represents a conservative estimate provided that systematic errors have been avoided. In view of the high quality of the applied transducers the measure-

ments of temperature and partial pressures are considered reliable and subject to only random errors. The quality of the kinetic measurements may be judged by comparison with computer simulations.

As input for our computer program we have chosen the following set of reactions where RH represents C_2H_6:

(1)	$H_2O^* \rightarrow H + OH$	$k_1 = 5.0 \times 10^5\ s^{-1}$
(2)	$H + H \rightarrow H_2$	$k_2 = 2.0 \times 10^9\ M^{-1}s^{-1}$
(3)	$H + OH \rightarrow H_2O$	$k_3 = 4.3 \times 10^9\ M^{-1}s^{-1}$
(4)	$OH + OH \rightarrow H_2O_2$	$k_4 = 4.3 \times 10^9\ M^{-1}s^{-1}$
(5)	$OH + RH \rightarrow H_2O + R$	$k_5 = 5.4 \times 10^8\ M^{-1}s^{-1}$
(6)	$OH + R \rightarrow ROH$	$k_6 = 1.0 \times 10^9\ M^{-1}s^{-1}$
(7)	$R + R \rightarrow R_2$	$k_7 = 1.0 \times 10^9\ M^{-1}s^{-1}$

Reactions (1) through (4) represent a simplified model for the radiolysis of pure water vapour. The formation of H and OH via excited water molecules in reaction (1) is chosen to represent the combined effect of all formation reactions including ion-molecule reactions like $H_2O^+ + H_2O \rightarrow OH + H_3O^+$ and the neutralization reaction $(H^+, nH_2O) + e^- \rightarrow H + n\ H_2O$. These reactions are very fast compared with the natural decay channels (2),(3) and (4) and the experimental rate of formation is well accounted for by the chosen value of k_1.

The formation and decay of OH is described by

$$d(OH)/dt = k_1(H_2O^*) - k_3(H)(OH) - 2k_4(OH)^2 - k_5(RH)(OH) - k_6(R)(OH).$$

With the chosen values of k_2, k_3 and k_4 we obtain good agreement with the experimental decay in pure water vapour, i.e. when

(RH)=0. After these primary adjustments we study the response of the model to changes in (RH) while $k_5 = 5.4 \times 10^8$ $M^{-1}s^{-1}$ is kept constant. As shown in Fig. 4 of A10 the model reproduces the complete set of experimental curves practically within the noise. Thus, the rate constant $k_5 = 5.4 \times 10^8$ $M^{-1}s^{-1}$ calculated on the basis of the simple analytical expressions (I) and (II) on p.36 is fully consistent with a model which takes into account also the non-trivial overlap between the source- and sink terms for hydroxyl radicals.

The absolute values of k_2, k_3 and k_4 are not known with certainty under our experimental conditions. Assuming that OH is consumed only via (3) and (4) in pure water vapour we find in accordance with the differential equation, $\tau = 1/(2k_4 + k_3)(OH)_o$. Based on ozone dosimetry (21a) and the reported radiolytic yields $G(O_3) = 12.8$ in pure oxygen (21b) and $G(OH) = 6.25$ in water vapour (9), we estimate an initial concentration of $(OH)_o = 1.24 \times 10^{-6}$ moles/liter. Combining this with the experimental half-life $\tau_o = 82$ μsec, we find a value of $2k_4 + k_3 = 9.8 \times 10^9$ $M^{-1}s^{-1}$. This value deviates by a factor of two from that reported by Gordon and Mulac (8) based on similar pulse-radiolysis experiments where they found $\tau_o = 50$ μsec and an estimated value of $(OH)_o = 10^{-6}$ moles/liter. It is not clear to us at the moment what causes this discrepancy but it seems most likely that the estimated values of $(OH)_o$ may be subject to errors. However, for the purpose of determining a reliable value of k_5 the absolute values of k_2,k_3, and k_4 are not of primary

importance as long as the value of $(2k_4 + k_3) \times (OH)_o$ used in the model is chosen in accordance with the experimental half-life.

The important conclusion of the computer simulations is that the set of experimental decay curves is well reproduced by the model only if $k_5 = (5.4 \pm 0.2) \times 10^8\ M^{-1}s^{-1}$. The value is most sharply defined at high (RH) where the decay is controlled almost exclusively by (5). Expressions (I) and (II) presented on p.36 can be used with confidence provided that the rate constants for the reactions

(3) $H + OH + M \rightarrow H_2O + M$

(4) $OH + OH + M \rightarrow H_2O_2 + M$

have reached the "second-order limit". At low partial pressures of the third body, M, the apparent second-order rate constants are porportional to the concentration of M, i.e. $k_4 = k_4^*(M)\ M^{-1}s^{-1}$ while at high partial pressures the rate constant approaches the second-order limit where k_4 remains constant. In gas mixtures, e.g. $Ar/H_2O/RH$ the components may have widely different third-body efficiencies, i.e. the value of k_4^* depends on the nature of M and the contributions from all species must be taken into account. Thus, the overall rate constant for a combination reaction may be written $k = \sum k_i(M_i)$. So in the "fall-off region" the apparent second-order rate constants may be rather complex functions of the gas composition. Under these circumstances the effect of an additive, e.g. RH, on the half-life of OH may be due to the "direct reaction" (5) but in addition RH may act as a third

body M=RH in all of the reactions (2),(3) and (4). Such a complex case may be very difficult to analyze. However, at high concentrations of RH reaction (5) results in a characteristic exponential decay while the third-body effect of RH has only little influence on the tail-end of the observed decay. Our experimental results show rather convincingly that the reaction OH + C_2H_6 -> H_2O + C_2H_5 is a "clean case" without interference from disturbing third-body effects. The value of k_5 obtained at 127°C can be taken with confidence and we apply the same procedures in our analysis of the experimental results obtained at lower temperatures.

10.1.2 Arrhenius Parameters OH + C_2H_6 -> H_2O + C_2H_5

Tables of experimental results obtained at different temperatures are collected in Appendix A10.1

At each temperature the experimental values of τ, dln(OH)/dt and (C_2H_6) were used with the analytical expressions (I) and (II) to calculate the value of k(OH+C_2H_6). The results are summarized below.

t	k(I)	k(II)	$k = Aexp(-E_a/RT)$
127	5.30×10^8	5.40×10^8	5.19×10^8
100	3.70×10^8	3.94×10^8	4.20×10^8
48	2.46×10^8	3.15×10^8	2.52×10^8
27	1.69×10^8	1.95×10^8	1.95×10^8
°C	$M^{-1}s^{-1}$	$M^{-1}s^{-1}$	$M^{-1}s^{-1}$

k(I) and k(II) are values of k(OH+C_2H_6) obtained by the two

different methods. The values obtained using expression (I) are in all cases lower than those obtained by expression (II). We believe that the method based on expression (II) is the most reliable because the full shape of the decay curve is utilized. The more primitive method based on expression (I) which utilizes only t(1/2) and t(1/4) is expected to underestimate the value of the rate constant because of contributions from build-up terms around the maximum of the decay curve. We have chosen to calculate the Arrhenius parameters using the values of k(II). Applying a simple least-square procedure to a plot of lnk(II) versus 1/T we obtain $A = 9.73 \times 10^9\ M^{-1}s^{-1}$ and $E_a = 2.33$ kcal/mole. The last column of the table displays calculated values of the rate constant using these values of (A,E_a). The reaction of hydroxyl radicals with ethane has been the subject of several investigations by different experimental methods over the past decade. In 1970 Greiner published an extensive study of Arrhenius parameters for OH + alkane reactions,(22). OH radicals produced by flash photolysis of water vapour were monitored by kinetic absorption spectrometry and the reaction rates were determined in the 300-500°K range. In the pulse-radiolysis work of Gordon and Mulac published in 1975 the reaction OH + C_2H_6 was studied only at 381°K and 416°K (8). Overend, Paraskevopoulos and Cvetanovic (1975) used flash photolysis combined with OH resonance absorption spectrometry to determine $k(OH+C_2H_6)$ at 295°K (23a). The latest contribution is due to Howard and Evenson (1976) who employed a discharge-flow reactor and detection of OH

radicals by laser magnetic resonance spectrometry in their study of OH + C_2H_6 at 296°K. (23b) A summary of the experimental results is given below.

A	E_a	$k(OH+C_2H_6)$	T	Reference
1.12×10^{10}	2.45	1.83×10^8	300	Greiner (22)
		4.00×10^8	381	Gordon and Mulac (8)
		4.80×10^8	416	
		1.59×10^8	295	Overend et al. (23a)
		1.75×10^8	296	Howard and Evanson (23b)
9.74×10^9	2.33	1.95×10^8	300	This work
$M^{-1}s^{-1}$	kcal/mole	$M^{-1}s^{-1}$	°K	

In view of the differences in techniques and experimental conditions the agreement between the results of the various groups is quite good.

10.1.3 Concluding remarks on $k(OH+C_2H_6)$

Our experimental results on the reaction OH + C_2H_6 -> H_2O + C_2H_5 studied in the temperature range T = 300 - 400°K is well accounted for by the Arrhenius expression

$$k(OH+C_2H_6) = 9.73 \times 10^9 \exp(-1173/T)\ M^{-1}s^{-1}$$

This corresponds to an activation energy of E_a = 2.33 kcal/mole. Our results are in fair agreement with the work of Greiner (22) who reported $k = 1.12 \times 10^{10} \exp(-1232/T)$ over the T=200-500 °K range.

10.2 OH + CFC-12 (CF_2Cl_2)

CFC12 is expected to be inert toward attack by hydroxyl radicals

because this compound is "perhalogenated" and abstraction of either F or Cl atoms are endothermic reactions due to the greater strength of C-F and C-Cl bonds relative to that of F-OH and Cl-OH bonds, respectively.

Therefore, we were somewhat puzzled by the experimental observation that the half-life of the OH-decay decreased with increasing CFC12 concentration.

Clearly, if this observation was due to a hitherto unexpected reaction channel it would alter the status of CFC12 (CF_2Cl_2) as one of the most critical compounds in the assessment of ozone depletion. We have considered the following hypothetical reactions:

(A) $CF_2Cl_2 + OH \longrightarrow CF_2Cl + ClOH$

(B) $CF_2Cl_2 + OH \longrightarrow CFCl_2 + FOH$

(C) $CF_2Cl_2 + OH \longrightarrow CF_2ClOH + Cl$

(D) $CF_2Cl_2 + OH \longrightarrow OCFCl_2 + HF$

As mentioned above the atom-transfer reactions (A) and (B) are endothermic to such an extent (20 kcal/mole) that they can certainly be neglected in the temperature range studied in this investigation, 300-400 K.

The displacement reaction (C) is exothermic by about 10 kcal/mole corresponding to the difference in bond energies, D(C-OH) - D(C-Cl). However, it is not easy to estimate the activation energy of such a reaction. Ionic displacement reactions in solution are well known but displacement reactions involving the OH-radical have not been reported.

The complex four-center elimination reaction (D) may be exother-

mic judging from the strength of the various bonds involved in the reaction.

The heat of reaction equals $D(FCl_2C-F) + D(O-H) - D(FCl_2C-O) - D(H-F)$ Two of these bond energies are known, $D(O-H) = 102$ kcal/mole and $D(H-F) = 135$ kcal/mole. We estimate $D(FCl_2C-F) = 105$ kcal/mole, a "standard value" of known C-F bonds. The remaining bond energy, $D(FCl_2C-O) = 90$ kcal/mole is a more dubious estimate.

However, these estimates indicate that the reaction (D) may be exothermic by about 18 kcal/mole.

Thus, it seems that reaction (C) and (D) cannot be ruled out on energetic grounds. The Arrhenius A-factors may be estimated using transition state theory but it is still beyond the capabilities of current theories to predict reliable activation energies.

In our analysis of the effect of CFC12 on the decay of OH we find that although the half-life decreases with increasing concentration the shapes of the individual decay curves remain non-exponential. Since any direct reaction like (C) or (D) would imply that the decay degenerates to a simple exponential curve: $(OH) = (OH)_o \exp(-k(CFC12)t)$, at sufficiently high CFC12 concentrations we conclude that the persistent second-order tail observed on all decay curves must be taken as evidence for a different type of reaction.

An obvious explanation would be that CFC12 acts as a very efficient third body M in the combination reaction, $OH + OH + M \rightarrow H_2O_2 + M$. This reaction has been investigated by

Black and Porter using flash photolysis combined with kinetic spectroscopy and relative thirdbody efficiencies for inert gases and a few simple molecules were reported. (24) However, CFC12 was not included in this investigation. In the low "low pressure limit" the apparent second-order rate constant will be proportional to the concentration of the third body. At higher concentrations of the third body the apparent second-order rate constant approaches a constant value, "the second-order limit".

Assuming a simple energy transfer mechanism where the third body removes excess vibrational energy from the new-born adduct molecule, we can obtain an analytical expression for concentration dependence of the apparent second-order rate constant:

(1) $OH + OH \rightarrow EX$

(2) $EX \rightarrow OH + OH$

(3) $EX + M \rightarrow H_2O_2$

Applying the steady-state approximation to the concentration of the vibrationally excited adduct (EX) we obtain $d(OH)/dt = -2k_1(OH)^2 k_3(M)/(k_2+k_3(M))$

Thus, for the reciprocal half-life we find

$$(I) \quad 1/\tau = 2k_1(OH)_o k_3(M)/(k_2+k_3(M))$$

which approaches a linear function in the low-pressure limit, i.e. when $k_3(M) << k_2$ and a constant second-order limit when $k_3(M) >> k_2$. We have applied expression (I) to a set of experimental OH half-lives measured at t = 75°C and with CFC12 concentrations in the range of 0 - 1.7 x 10^{-3} moles/liter.

We obtained the best fit between (I) and the experimental values using $2k_1(OH)_o = 7.75 \times 10^4$ as the second-order limit and $k_3(M)/k_2 = 0.15 + 380(CFC12)$ to account for the concentration dependence. The constant term of 0.15 is assigned to the contribution from argon and water vapour present in constant concentrations.

The excellent fit between the experimental half-lives and those calculated using the analytical expression (I) is shown in Fig. 5. Further support for this energy transfer mechanism was obtained by computer simulations of the complete set of reactions involved. The model curves reproduce not only the experimental half-life but also the persistent second-order tail as shown in Fig. 6. Thus the simple model of energy transfer from a vibrationally excited adduct to a colliding third body account for all of the characteristic kinetic features of the experimental OH decay curves. However, we have to consider some important implications of the proposed model. First of all, if the interpretation is correct it means that OH combination reactions have not reached the second-order limit in a system containing 35 torr of water vapour and backed up by argon to 1 atm. at 75°C.

Increasing concentrations of CF_2Cl_2 cannot be ascribed to a simple third-body effect on the OH combination rate constants. However, in view of the great succes of the energy transfer model in accounting for the observed kinetic features we consider the possibility of the high specificity of different third bodies (H_2O and CF_2Cl_2) on the two combination reactions:

(a) $H + OH + M \rightarrow H_2O$

(b) $OH + OH + M \rightarrow H_2O$

In terms of the energy transfer model we have to consider the deactivation of the vibrationally excited molecules.

(c) $(H_2O) + M \rightarrow H_2O \qquad \nu(H - OH) = 3657\ cm^{-1}$

(d) $(H_2O) + M \rightarrow H_2O \qquad \nu(HO - OH) = 890\ cm^{-1}$

The water molecule may be a very efficient third body in (c) because of near-resonant transfer of vibrational energy between identical oscillators.

On the other hand, the water molecule has no vibrational mode matching the hot 890 cm^{-1} mode to be deactivated in (d).

While H_2O may have a relativity low third-body efficiency with respect to reaction (d) it seems that resonance transfer is possible in the case of CF_2Cl_2, which has a strong combination mode near 890 cm^{-1}. Thus, it seems possible that the H_2O and CF_2Cl_2 act almost exclusively as specific resonance in enhanced chaperon molecules in the specific reactions (c) and (d), respectively.

The proposed model also implies high values of the combination rate. Based on ozone dosimetry and assuming that the yield of hydroxyl radicals in H_2O/Ar-mixtures is the same as in pure water vapour, G(OH) = 6.25 we estimate an initial concentration of $[OH]_o = 10^{-10}$ moles/liter. Using this value we find

$$2k(OH+OH) + k(H+OH) = 7.75 \times 10^{10}\ M^{-1}s^{-1}$$

The relative magnitude of the two rate constants is unknown, but assuming that they are equal we obtain

$$2k(OH+OH) = k(H+OH) = 2.6 \times 10^{10}\ M^{-1}s^{-1}$$

This is a high value but not unrealistic for radical combina-

tion reactions which do not require any activation energy.
We conclude that the interpretation of the experimental data on Ar-H_2O-CF_2Cl_2in terms of the "third-body energy transfer model" is well supported by the great success of the simple analytical expression (I) as well as complete computer simulations in accounting for all of the characteristic kinetic feature observed in the experimental OH decay curves.
The implied resonance-enhanced vibrational energy transfer is a well-known effect which has been observed experimentally in a number of systems.
Finally, the estimated absolute values of rate constants for the H+OH and OH+OH combination reactions are within a range compatible with realistic collision cross-sections.
The present investigation involves only studies of OH radical kinetics without attemps to analyse the distribution of stable products. An important implication of the proposed model is that the yield of H_2O_2 should increase with increasing concentration of CF_2Cl_2.
Thus, studies of the yield of H_2O_2 might serve as an unambigeous test of the model. This has not been attempted because of expected difficulties in the analysis of H_2O_2 which to a large extent may be lost by adsorption and catalytic decomposition on the walls of the stainless steel irradiation cell.
<u>Alternative mechanism: DIRECT EXCITATION</u>.
We have considered an alternative complex mechanism involving dissociation of CF_2Cl_2 in competition with the primary water dissociation which is supposed to occur via energy transfer

from excited argon atoms.

(E1) $Ar^* + H_2O \rightarrow Ar + H + OH$

(E2) $Ar^* + CF_2Cl_2 \rightarrow Ar + CF_2Cl + Cl$

In additions to (E2) other possible fragmentation reactions may be considered.

The relative yields of atoms and radicals originating from (E2) are proportional to the ratio $K_{E2}[CF_2Cl_2]/k_{E1}[H_2O]$.

Asumming that the rate constants are nearly equal ($k_{E1} = k_{E2}$), we may expect a significant yield from (E2) when the concentration of CF_2Cl_2 approaches or exceeds that of the water vapour.

The fragments produced in (E2) may all react with the OH radicals and the effect would be a shorter OH half-life and complex secondorder kinetics, as observed experimentally.

However, based on computer simulations we find that the "direct excitation model" cannot account for the shape of the experimental $1/\tau$ versus $[CF_2Cl_2]$ curves.

The significant difference is that the model implies a positive second derivative of $1/\tau$ versus $[CF_2Cl_2]$ while the experimental curvature corresponds to a negative second derivative.

The clear failure of the simulated DIRECT EXCITATION MODEL in accounting for the experimental kinetic features shows that major contributions from (E2) can be ruled out.

Therefore, we believe that it is safe to retain the interpretation based on the "THIRD-BODY ENERGY TRANSFER MECHANISM" which proved consistent with all the experimental observations.

Summary.

The most important conclusion regarding the tropospheric lifetime of CF_2Cl_2 is that this compound appears to be completely inert toward attack by OH radicals, even at atmospheric pressures where complex reactions like displacement (3) and elimination (4) might become feasible because of "pressure stabilization" of an intermediate complex. We feel that the present "high-pressure investigation" rules out the occurrence of such reactions.

To estimate an upper limit for the rate of any direct reaction, (5) OH + CF_2Cl_2 -> products, we calculate an "apparent rate constant" of $k_{app} = 1.4 \times 10^7$ $M^{-1}s^{-1}$ corresponding to the initial slope of the experimental $1/\tau$ versus (CF_2Cl_2) curve.

Our computer analysis showed that the major part, if not all, of the change in experimental half-lives must be ascribed to third-body assisted combination reactions of H and OH.

The good signal-to-noise ratio of the individual OH decay curves indicates that a 10% contribution from a pseudo-first-order decay channel (5) should be clearly observable on the tail-end of the decay curve. Since the simulated curves based on the energy transfer model matches the experimental decay curves very closely, even at the tail-end, we estimate $k(OH + CF_2Cl_2) < 0.1 \times k_{app} = 1.4 \times 10^6$ $M^{-1}s^{-1}$. This figure is in agreement with previous experimental results obtained with low-pressure techniques. (5)

Thus, reaction with hydroxyl radicals is not a probable sink

for CF_2Cl_2 and a very long tropospheric lifetime is to be expected for this compound.

Therefore the continued release of large amounts of CF_2Cl_2 and other antropogenic halocarbons must be considered a potential threat to the stability of the stratospheric ozonelayer.

10.3 The reaction $OH + CH_4 \rightarrow H_2O + CH_3$

Tables of experimental results obtained at different temperatures are collected in Appendix A10.3.

At each temperature the rate constant was calculated by the procedure described in Part 10.1 (p.36), i.e. based on the expression

(II) $$- d\ln(OH)/dt = I_o + k(RH)$$

where $k = k(OH+CH_4)$ and $(RH) = (CH_4)$. In the presence of methane plots of ln(OH) versus time were linear in accordance with (II). For a set of such decay curves the slopes were plotted versus (CH_4). A summary of the experimental results is presented below.

t	$k(OH+CH_4)$	$p(CH_4)$	no. of exp.
27	$(1.9\pm0.2)\times10^7$	$0-3.25\times10^{-2}$	17
48	$(2.0\pm0.2)\times10^7$	$0-4.10\times10^{-2}$	11
72	$(2.5\pm0.3)\times10^7$	$0-1.00\times10^{-2}$	8
75	$(2.4\pm0.2)\times10^7$	$0-1.06\times10^{-1}$	17
100	$(3.0\pm0.2)\times10^7$	$0-9.04\times10^{-2}$	25
127	$(3.5\pm0.5)\times10^7$	$0-5.50\times10^{-2}$	12
^oC	$M^{-1}s^{-1}$	atm	90

The results may be presented in terms of the Arrhenius expression

$k = A\exp(-E_a/RT) = 2.32\times10^{8}\exp(-765/t)$

This equation implies an activation energy of E_a = 1.52 kcal/mole which is in serious disagreement with the results of previous studies, E_a = 3.77 kcal/mole (ref.22) and E_a = 3.92 kcal/mole (ref.25).

Such a large discrepancy indicates a systematic error source which is common to all of the experimental results on the reaction $OH + CH_4 \rightarrow H_2O + CH_3$.

The presence of even small amounts of a highly reactive impurity in the applied methane would give rise to a higher apparent rate constant,

$$k^* = k_1 + k_2(I)/(CH_4).$$

If $k_1 = k(OH+CH_4) = 6\times10^{6}\ M^{-1}s^{-1}$ at 300 K (ref.22) and we assume that the impurity reacts with a rate constant of $k_2 = 10^{10}\ M^{-1}s^{-1}$, we find that $k^* = 2\times k_1$ when $(I)/(CH_4) = 6\times10^{-4}$, i.e. at an impurity level of only 0.06%.

According to a careful analysis by gas chromatography the applied methane contained 0.13% C_2H_6 and 0.18% C_2H_4 plus about 0.08% of $(H_2+Ar+N_2+O_2)$. Since $k(OH+C_2H_6) = 5.4\times10^{8}M^{-1}s^{-1}$ the contribution from 0.13% ethane amounts to only about a 10% increase in the apparent rate constant. However, ethylene is a much more reactive impurity, $k(OH+C_2H_4) = 3.4\times10^{9}M^{-1}s^{-1}$ at 300 K. (ref.5) and in the presence of 0.18% C_2H_4 we expect to find $k^* = k_1 + 6.12\times10^{6}\ M^{-1}s^{-1}$.

Clearly, in experiments with (CH_4 + 0.18% C_2H_4) the impurity

accounts for an apparent rate constant which is much higher than the true value of $k(OH+CH_4)$.

Our neglect of elementary precautions with respect to impurities is highly regrettable. We conclude that all of the 90 experimental results on $OH+CH_4$ must be rejected only because of the very reactive impurity found in the applied methane. We shall repeat the experimental work using 99.995% CH_4.

10.4 The reaction $OH + CH_3Cl \rightarrow H_2O + CH_2Cl$

In studies of additives like CH_3Cl which react fairly slowly with hydroxyl radicals it may be necessary to apply rather high partial pressures of the additive in order to drive the title reaction, i.e. to obtain a significant change in the decay rate.

In particular at room temperature where the saturation pressure of water vapor is rather low an increase in the decay rate may only be observed if the partial pressure of the additive approaches that of the water pressure. Under these circumstances there is a risk of direct fragmentation of CH_3Cl by ionization or energy transfer from the primary ionic and excited species which are produced by the ionizing radiation. If a significant amount of such fragments are formed along with the OH radicals it becomes a hopeless task to exctract the effect of the title reaction from the combined effect of all other radical-radical reactions. We consider the reactions:

(1) $Ar^* + H_2O \rightarrow Ar + H + OH$

(2) $Ar^* + CH_3Cl \rightarrow Ar + CH_3 + Cl$

(3) $H + H + M \rightarrow H_2 + M$

(4) $OH + H + M \rightarrow H_2O + M$

(5) $OH + OH + M \rightarrow H_2O_2 + M$

(6) $OH + CH_3Cl \rightarrow H_2O + CH_2Cl$

(7) $OH + CH_2Cl \rightarrow P$

(8) $2\ CH_2Cl \rightarrow C_2H_4Cl_2$

---

(9) $OH + CH_3 \rightarrow CH_3OH$

(10) $OH + Cl \rightarrow HOCl$

We assume that the primary radicals are produced via excited argon atoms (Ar*). The formation of CH_3 and Cl via (2) can only be avoided if $k_1(H_2O) >> k_2(CH_3Cl)$. We assume that this condition is fulfilled in experiments where the initial yield of OH is the same as that observed in the pure OH/Ar system, i.e. when $(CH_3Cl)=0$.

In experiments at room temperature we observed a significant reduction of the initial yield of OH when $(CH_3Cl) > 0.5\ (H_2O)$. This was taken as strong evidence for the occurance of reaction (2). Such experiments were rejected because of the difficulties in evaluating the contributions from the consecutive reactions (9) and (10).

In our analysis of the kinetic results we most often apply plots of ln(OH) versus time which become near linear in the limit of high concentrations of the additive where the title reaction controls the decay rate. Deviations from the simple behavior are observed when radical-radical reactions are important.

For the characteristic derivative we use the short-hand notation $\alpha = - d\ln(OH)/dt$ and likewise RH = CH_3Cl and R

= CH_2Cl. The decay of OH via (4),(5),(6),(7),(9) and (10) is then described by

$$(I)\quad \alpha = k_4(H) + 2k_5(OH) + k_6(RH) + k_7(R) + k_9(CH_3) + k_{10}(Cl)$$

If $k_1(H_2O) >> k_2(RH)$ reaction (2) is unimportant and therefore we can neglect also (9) and (10). (I) is then reduced to

$$(II)\quad \alpha = k_4(H) + 2k_5(OH) + k_6(RH) + K_7(R)$$

For the initial slope at t=0 we have $(H)_o=(OH)_o$ and (R)=0 and we obtain the very simple expression

$$(III)\quad \alpha_o = (k_4+2k_5)(OH)_o + k_6(RH)_o$$

It seems quite obvious that the safest procedure is to utilize the initial slope which contains no contribution from the consecutive reaction (7). Since all experiments were carried out using the same initial concentration of hydroxyl radicals $(OH)_o$ the leading term in expression (III) remains constant and the unknown rate constant equals the slope of the plot of α_o versus $(RH)_o$ for a series of experiments covering a range of additive concentrations.

Tables of experimental results are collected in Appendix A10.4. A summary is presented below.

t	k(OH+CH_3Cl)	p(CH_3Cl)	no. of exp.
27	$(4.3\pm0.5)\times10^7$	$0-2.0\times10^{-2}$	14
48	$(4.7\pm0.5)\times10^7$	$0-2.8\times10^{-2}$	11
72	$(6.4\pm0.5)\times10^7$	$0-2.0\times10^{-2}$	12
100	$(7.8\pm0.8)\times10^7$	$0-4.2\times10^{-2}$	11
127	$(9.2\pm0.9)\times10^7$	$0-2.0\times10^{-2}$	8
^oC	$M^{-1}s^{-1}$	atm	56

The results may be expressed in terms of the Arrhenius expression

$$k = A\exp(-E_a/RT) = 1.07\times10^9\exp(-976/T)\ M^{-1}s^{-1}$$

corresponding to an activation energy of $E_a = 1.94\pm0.10$ kcal/mole. Jeong and Kaufman (25) has investigated the reaction using a discharge-flow reactor and resonance fluorescence detection of OH.

They report $k = 2.11 \times 10^9 \exp(-1314/T)\ M^{-1}s^{-1}$ corresponding to $E_a = 2.61\pm0.10$ kcal/mole.

In our opinion the work of Jeong and Kaufman (25) represents the most extensive and reliable study on OH + halogenated hydrocarbons reporteds so far. Since they covered a wide range of temperatures the uncertenties in the reported activation energies are expected to be low. Therefore we are not quite happy about our value of the activation energy, $E_a = 1.94$ kcal/mole which is substantially lower than the value reported by Jeong and Kaufman.

At 127^oC our value of k(OH+CH_3Cl) $= 9.2\times10^7\ M^{-1}s^{-1}$ is in fair

agreement with Jeong and Kaufmans value (7.9×10^7 $M^{-1}s^{-1}$). However at 27°C our value of $k=4.3 \times 10^7$ $M^{-1}s^{-1}$ would seem to be overestimated by a factor of 1.7.

In our experimental work we expected troublefree performance at the higher temperatures where we could apply fairly high partial pressures of water vapor. This is important to fulfill the requirement stated above $k_1(H_2O) >> k_2(RH)$ to prevent the occurance of (2). At the higher partial pressures of water vapor we should also be safe regarding the value of the apparent second order rate constants k_4 and k_5 which should attain the limiting high pressure value.

At room temperature we may expect two kinds of difficulties because of the low saturation pressure of water vapor. When the rate constant of the title reaction is of the order of 10^7 $M^{-1}s^{-1}$ we have to apply p(RH) = 10 torr in order to reduce the OH half-life by a factor of two relative to the "natural half-life" $\tau_o = 10^{-4}$ sec. Already at this partial pressure we begin to observe a reduction of the initial yield of OH due to competition between reactions (1) and (2). This means that the initial value of the derivative α contains a small but ill-defined contribution from the reactions (9) and (10). The most serious difficulty in our studies of the reaction rates at room temperature is perhaps that the rates of the termolecular reactions (4) and (5) may be somewhat dependent on the partial pressure of the reactive additive. This means that in expression (III) at p.57 the leading term $(k_4+2k_5)(OH)_o$ does not remain constant because

both of the apparent second order rate constants k_4 and k_5 depend on the partial pressures of all of the species present including the reactive additive RH.

Our experiments with CFC-12 showed beyond any reasonable doubt that the half-life of OH decreased with increasing values of (CF_2Cl_2) but the decay remained second order (long tail) with an apparent rate constant $k = k_{max}(X/(1+X))$ where $X = 0.15 + 380(CFC-12)$. In the experiments with CH_3Cl we may expect a similar effect of the additive which act as a third body $M=CH_3Cl$ to speed up the reactions (4) and (5) in competition with the title reaction (6).

Thus, the apparent rate constant k_6 as derived from expression (III) will have to be corrected for this "third-body effect". Unfortunately, since different third bodies may have very different efficiencies we cannot apply the analytical expression derived for (CFC-12) which seems to be a very effective third body, presumably due to a resonance effect. Thus we cannot assume that CH_3Cl has the same efficiency and therefore it is not obvious how to correct for the third-body effect. We do have some experimental evidence for the third-body effect from the analysis of the curvature of the semi-logaritmic plots.

According to (II) the slope at the tail-end of the decay is determined mainly by the term $k_6(RH)$. At 27°C and $p(CH_3Cl) = 7$ torr we observed that the difference between the inital and the final slope exceeded the value of $(k_4+2k_5)(OH)_o$ obtained in a reference experiment with (RH)=0. Clearly, at

27°C the observed increase in the decay rate upon addition of small amounts of CH_3Cl is largely due to the title reaction but with contributions from radical-radical reactions which are not easily corrected for.

We believe that these difficulties which are most disturbing at low temperatures may be eliminated by chosing different experimental conditions and by studying the effect of varying $(OH)_o$. This is easily done simply by varying the irradiation dose. By varying maximum concentration of OH and the other free radials we get information about the radical-radical reactions which interfere with the title reaction. The main problem is that OH disappears by a number of parallel reactions We think that a simultaneous measurement of the formation of the secondary radical R would be a great advantage in the analysis of the kinetics. This is experimentally feasible in the case of Methane, $OH + CH_4 \rightarrow H_2O + CH_3$ where the formation of CH_3 can be followed by monitoring the characteristic absorption at 216 nm.

In the present series of experiments we discovered that some of the halogenated metyhyl radicals like CCl_3 posses absorption bands in the range of 200-220 nm.

We shall take advantage of these findings in future experiments...

10.5 The reaction $OH + CH_2Cl_2 \rightarrow H_2O + CHCl_2$

Tables of experimental results obtained at five different temperatures are collected in appendix A10.5. A summary is presented below.

t	$k(OH+CH_2Cl_2)$	k(I)	k(25)
27	1.4×10^8	0.98×10^8	1.05×10^8
49	1.3×10^8	1.26×10^8	1.34×10^8
75	1.5×10^8	1.63×10^8	1.70×10^8
97	2.0×10^8	1.98×10^8	2.04×10^8
127	2.5×10^8	2.48×10^8	2.52×10^8
^oC	$M^{-1}s^{-1}$	$M^{-1}s^{-1}$	$M^{-1}s^{-1}$

Our experimental values of $k(OH+CH_2Cl_2)$ are listed in the left-hand column. The "odd value" $k = 1.4 \times 10^8$ $M^{-1}s^{-1}$ obtained at 27°C seems completely out of line compared with the rest of the series.

In the experimental work liquid CH_2Cl_2 was injected through a septum into the reaction vessel. As the boiling point of CH_2Cl_2 is 40.5°C it seems likely that measurements of the partial pressure at 27°C may have been made too quickly before complete evaporation of the liquid. Omitting the k-value at 27°C and applying a linear least square fit to lnk versus 1/T we obtain the Arrhenius expression:

$$(I) \quad k(OH+CH_2Cl_2) = A\exp(-E_a/RT) = 4.05 \times 10^9 \exp(-1117/T)\ M^{-1}s^{-1}$$

Using this expression we calculated the values of k(I) shown in the center column. Our experimental results are in good agreement with those of Jeong and Kaufman (25) shown in the column to the right. In the table below the rate parameters obtained in the present work are compared with the results of previous investigations.

k(298 K)	A	E_a	T range	References
0.95×10^8	4.05×10^9	2.22	322-400	This work
1.03×10^8	3.45×10^9	2.08	251-455	25
0.70×10^8	2.57×10^9	2.17	245-375	26
0.87×10^8				27
0.93×10^8				28
$M^{-1}s^{-1}$	$M^{-1}s^{-1}$	kcal/mole	^oK	

The agreement between the reported rate constants at T = 298^{o}K is quite satisfactory. However, the results of Davis et al. (26) appear to be about 25% lower than the average of the other measurements throughout the range of T = 245-375^{o}K. The activation energies are in agreement within 3% of the simple average value, E_a = 2.16 kcal/mole. Thus, it would seem reasonable to combine the average value of the rate constants measured at room temperature, k(298) = 8.96×10^7 $M^{-1}s^{-1}$ with the average value of E_a = 2.16 kcal/mole to evaluate an Arrhenius expression which takes into account all of the available data:

$$k(OH+CH_2Cl_2) = 3.41 \times 10^9 \exp(-1085/T)\ M^{-1}s^{-1}$$

The A-factor in this expression is almost identical with that reported by Jeong and Kaufman who covered a large range of temperatures in their experimental work. This is of course necessary in order to obtain a reliable value of the A-factor.

10.6 The reaction $OH + CHClF_2 \rightarrow H2O + CClF_2$ (CFC-22)

Tables of individual experimental results obtained at five different temperatures are collected in appendix A10.6. A summary is presented below.

t	k(OH+$CHClF_2$)	k(I)	k(25)
27	3.1×10^6	2.9×10^6	2.9×10^6
52	4.0×10^6	4.6×10^6	4.5×10^6
76	6.4×10^6	6.7×10^6	6.4×10^6
105	1.0×10^7	9.9×10^6	9.3×10^6
127	1.3×10^7	1.3×10^7	1.2×10^7
^oC	$M^{-1}s^{-1}$	$M^{-1}s^{-1}$	$M^{-1}s^{-1}$

A linear least square fit of the experimental values (left column) versus 1/T yields an Arrhenius expression

(I) $k(OH+CHClF_2) = Aexp(-E_a/RT) = 1.12 \times 10^9\ M^{-1}s^{-1}$

corresponding to an activation energy of E_a = 3.55 ± 0.30 kcal/mole The values in the center column are calculated using expression (I). Our experimental values are in good agreement with the results of Jeong and Kaufman (25) shown in the right-hand column. Our results would seem to indicate a higher activation than that reported in ref 25, E_a = 3.32 kcal/mole. However, the difference is smaller than the estimated uncertainty. $CHClF_2$ is an important refrigerant (CFC-22) and its reaction with OH has been subject to several previous investigations. It is interesting to compare all of the data available at present.

Rate parameters for the reaction $OH + CHClF_2 \rightarrow H_2O + CClF_2$

k(298 K)	E	T range	References
2.9×10^6	3.25	297-434	29
2.1×10^6			28
2.9×10^6	3.13	250-350	30
2.6×10^6	3.29	253-427	31
2.8×10^6	3.54	263-373	32
2.0×10^6	4.60	294-426	33
2.8×10^6			34
2.9×10^6	3.32	293-482	25
2.9×10^6	3.55	300-400	This work
$M^{-1}s^{-1}$	kcal/mole	^oK	

With the exception of E_a = 4.60 kcal/mole reported by Clyne and Holt (33) the experimental values of the activation energy are in good agreement and with an average value of E_a = 3.35 kcal/mole. Combining this value with the avarage value of $k(298^oK) = 2.74 \times 10^6\ M^{-1}s^{-1}$ we obtain

$$k(OH+CHClF_2) = 7.85 \times 10^8 \exp(-1686/T)\ M^{-1}s^{-1}$$

This expression accounts well for all of the available experimental results in the range of T = 250-427 ^oK. The agreement between the results is quite encouraging in view of the differences in experimental techniques and ranges of pressures applied by the various groups.

10.7 The reaction OH + $CHCl_3$ -> H_2O + CCl_3

Tables of experimental results are collected in Appendix A10.6. A summary is presented below.

t	k(OH+$CHCl_3$)	p($CHCl_3$)	no. of exp.
27	1.8 x 10^8	0-9.5x10^{-3}	20
48	1.8 x 10^8	0-5.8x10^{-3}	7
72	2.4 x 10^8	0-8.4x10^{-3}	8
97	1.7 x 10^8	0-9.1x10^{-3}	8
127	2.2 x 10^8	0-7.4x10^{-3}	8
^oC	$M^{-1}s^{-1}$	atm	51

The experimental results exhibit an irregular pattern without any clear trend regarding the expected temperature dependence. The values obtained at the higher temperatures 97-127^oC look reasonable when compared with rate constants reported by Jeong and Kaufman (25) who found k = 1.8 x 10^8 $M^{-1}s^{-1}$ at 127^oC. However, our value at 27^oC is almost a factor of three higher than that reported in ref.25. This large discrepency would seem to indicate that in our experiments at 27^oC more than 50% of the OH radicals disappear via other reactions competing with the title reaction, OH + $CHCl_3$ --> H_2O + CCl_3.
The consecutive reaction OH + CCl_3 --> Product does not contribute to the initial decay rate because [CCl_3] = 0 when t = 0 The high-purity sample of $CHCl_3$ applied in our experiments was analyzed by gas chromatography and mass spectrometry and

the total impurity level was found to be less than 0,01%. Assumming a maximum rate constant of k(OH + impurity) = $10^{10}M^{-1}s^{-1}$ the contribution from the impurity to the observed rate constant amounts to less than 1.4% if the "true value" of k(OH + $CHCl_3$) = $7x10^{7}M^{-1}s^{-1}$ as reported in ref 25. Thus the increased decay rate of OH observed at the lower temperatures cannot be explained by the impurity level of <0.01% in the applied $CHCl_3$.

Fragmentation of $CHCl_3$ by attack of primary species (Ar^*,Ar^+,e^-) becomes important when the ratio $p(CHCl_3/p(H_2O)$ increases beyond a critical value.

Experimentally we found that the yield of OH remains constant when $p(CHCl_3)/p(H_2O) < 1/20$. However, in our experiment at 27°C with $p(H_2O)$ = 20 mbar and $p(CHCl_3)$ = 2.9 mbar we observed that the initial yield of OH, monitored at the end of the irradiation pulse, the maximum value was reduced to 76% of the maximum value measured in the absence of $CHCl_3$. It seems obvius that the missing 24% of the OH radicals are replaced by fragtments of $CHCl_3$ formed by reactions with primary ionic and excited species i.e. Ar^*,$Ar^+$and e^-. Fragmentation into Cl + $CHCl_2$, H + CCl_3 and HCl + CCl_2 takes place during the decay of the shortlived primary species. The simultanious formation of OH along with the secondary atoms and radicals H,Cl,CCl_3,etc. implies a number of unwanted side reactions of OH competing with the title reaction. All of these reactions contribute to the initial decay rate because the secondary radicals are formed during the early event. During the experi-

mental work we were of course aware of this posibility, but the observation of simple exponential OH decay curves made us believe that the decay rate was determined almost exclusively by the title reaction. Computer simulation showed that this was a simple-minded conclusion. Actually, near-exponential decay curves may be observed in cases, when 50% of the over-all decay rate is due to radical-radical reactions. We realize that the experimental data base available at present does not allow us to make the proper corrections for the contribution from side reactions to the over all rate constant. Based on these experiments we have defined some important requirements of future experiments on OH + $CHCl_3$.

(1) To prevent direct fragmentation of $CHCl_3$ all experiments should be carried out using $p(CHCl_3)/p(H_2O) < 0.1$

(2) The kinetics should be studied as a function of two parameters $(OH)_o$ and $(RH)_o$.

(3) Simultaneous studies of OH-decay and CCl_3-formation.

Using this strategy we are pretty convinced that any reaction competing with the title reaction $OH + CHCl_3 \rightarrow H_2O + CCl_3$ can be quantitatively accounted for.

10.8 The reaction $OH + CH_3CCl_3 \rightarrow H_2O + CH_2CCl_3$

Tables of individual experimental results are collected in appendix A10.8. A summery is given below.

t	k(OH + CH_3CCl_3)	Comments
27	3.5×10^8	Not purified
48	2.4×10^8	After destillation
75	2.1×10^8	-"-
100	2.0×10^8	-"-
127	2.4×10^8	-"-
127	2.8×10^8	-"-
127	3.4×10^8	Not purified
^oC	$M^{-1}s^{-1}$	

Our experimental results are in seroius disagreement with those of previous investigations. Howard and Evenson (23b) reports $k = 9.0 \times 10^6$ $M^{-1}s^{-1}$ at 296°K in close agreement with the value obtained by Davis et al. (26)

In our first experiment we used a sample of 95% $CHCCl_3$ (FLUKA) without purification. The high values of the apparent rate constant indicated the presence of a highly reative impurity. By gaschromatography we found as much as 4% of the most abundant impurity while other impurities we present in much smaller concentrations After distillation we still obtained too high values of the apparent rate constant and we conclude that the reactive impurity is difficult to remove. A mass spectrum of the distilled sample was obtained but we were not able to identify the impurity. In view of the high reactivity is seems likely that the impurity is an unsatuated compound, e.g. CH_2CCl_2. We have postponed further experimental work on methyl-chloroform until an ultra-pure sample has become available.

11. SUMMARY

Kinetics of the reaction of Hydroxyl Radicals with Methane, Ethane and a series of Cl- and F-substituted Methanes and Ethanes was studied by pulse radiolysis of water vapor in the presence of varying amounts of reactant molecules. The kinetics was followed by monitoring the transient absorption of the $OH(X^2\Pi\text{-}A^2\Sigma^+)$ transition. The experimental results are summarized below.

Rate parameters for the reaction $OH + RH \rightarrow H_2O + R$

Reactant	$k(OH+RH)_{300}$	A	E_a	Comments
CH_4	rejected			Impurities (a)
CH_3Cl	4.3×10^7	1.07×10^9	1.94	
CH_2Cl_2	1.0×10^8	4.05×10^9	2.22	
$CHCl_3$	rejected			Exp. cond. (b)
$CHFCl_2$	2.9×10^6	1.12×10^9	3.55	
CF_2Cl_2	$<< 10^6$			CFC-12 unreactive
C_2H_6	2.0×10^8	9.73×19^9	2.33	
CH_3CCl_3	rejected			Impurities (a)
Units	$M^{-1}s^{-1}$	$M^{-1}s^{-1}$	kcal/mol	

(a) Experimental data rejected due to reactive impurities

(b) Contributions from direct fragmentation of $CHCl_3$

The values of $k(OH+RH)_{300}$ are absolute bimolecular rate constants in units of liter x $mole^{-1}$ x s^{-1} ($M^{-1}s^{-1}$, measured at 27°C (T=300K).

The Arrhenius parameters (A, E_a) listed in the two columns to the right were derived from the observed temperature dependence of the rate constants determined at five different temperatures in the range of t = 27 - 127°C. In this temperature range the expression $k = A\exp(-E_a/RT)$ $M^{-1}s^{-1}$ accounts for all of the experimental results within an estimated error limit of ± 10%.

Our experimental results are in good agreement with the Arrhenius parameters reported in the work of Jeong and Kaufman (25), which in our opinion represents one of the most competent recent contributions on OH radical kinetics.

Using a discharge-flow resonance fluorescence apparatus Jeong and Kaufman studied the reactions of hydroxyl radicals with methane and nine Cl- and F-substituted methanes at a pressure of about 3 torr and over a temperature range of T = 250-490 °K. The primary advantage of this technique is that the reaction of interest (e.g. $OH+CH_4$) can be studied practically without interference from competing radical-radical reactions which are almost completely suppressed because of the low pressure and the very low steady state concentrations of OH. Minor losses of OH in wall reactions were taken into account and it appears that other possible systematic error sources were eliminated. The activation energies obtained in this work are expected to be very accurate in view of the large temperature range covered. Therefore we find it very satisfactory that our experimental results agree with those of Jeong and Kaufman within the experimental uncertainties. This

proves that our pulse radiolysis technique can be used to obtain reliable rate constants for OH + RH elementary reactions which occur along with unavoidable, simultaneous and consecutive radical-radical reactions

It also means that the analytical procedures applied in the calculation of rate constants can be used with confidence, provided that certain constraints on the experimental conditions, e.g. concentration ratios, are taken into accounts.

11.2 Theoretical considerations

An important objective of the present investigation was to study the effect of halogen substitution on the rate of H-atom abstraction by OH radicals, R-H + OH -> R + H-OH. Considering the series

RH	CH_4	CH_3Cl	CH_2Cl_2	CH_3Cl_3
k(300°K)	4.7×10^6	2.6×10^7	1.1×10^8	6.6×10^7 $M^{-1}s^{-1}$

it is quite obvious that Cl-substitution speeds up the reaction. The maximum rate constant is that of OH + CH_2Cl_2, i.e. the increase is not a monotoneous function of the Cl-substitution. It is of interest to study the effect of halogen substitution on each of the Arrhenius parameters A and E_a, respectively. In the case of alkanes C_nH_{2n+2} Greiner (22) has established simple additivity rules for primary, secondary, and tertiary C-H bonds. The overall rate constant is obtained by summing up the individual contributions:

$$k = N_1k_1 + N_2k_2 + N_3k_3$$

$$= 6.14 \times 10^8 N_1 \exp(-1635/RT) + 1.41 \times 10^9 N_2 \exp(-850/RT) + 1.26 \times 10^9 N_3 \exp(+190/RT)$$

where N_1, N_2, and N_3 are the numbers of primary, secondary, and tertiary C-H bonds, respectively. The apparent negative activation energy, E_3 = -190 cal/mole for the abstraction from tertiary C-H bonds was replaced by E_3 = 0 in a revised expression which fits the available literature values of k(OH+RH) within ± 20% at T = 300-500°K. (5) The simple formula established by Greiner is valid only for the higher alkanes (n>2), i.e. with the exception of CH_4 and C_2H_6. Regarding the halogensubstituted methanes the Arrhenius parameters for the reaction with hydroxyl radicals exhibit an irregular pattern.

R-H + OH -> R + H-OH

RH	A	A/N_H	E_a	D(R-H)	q
CH_4	3.37×10^9	0.84×10^9	3.92	105	12
CH_3Cl	2.11×19^9	0.70×10^9	2.61	103	14
CH_2Cl_2	3.45×10^9	1.73×10^9	2.08	101	16
$CHCl_3$	3.40×10^9	3.40×10^9	2.35	95	22
	$M^{-1}s^{-1}$	$M^{-1}s^{-1}$	kcal/mol	kcal/mol	kcal/mol

We notice that the A-factor per equivalent H-atom (A/N_H) is neither a constant nor a monotoneous function of the Cl-substitution.

For a series of similar reactions Evans and Polanyi (36) established a simple correlation between activation energy (E_a) and the heat of reaction (q):

(E-P) $$E_a = E_o - \alpha q$$

where E_o and α are empirical constants.

In the right-hand column we have calculated the heats of reaction, q = D(H-OH) - D(R-H) using D(H-OH) = 117 kcal/mol and values of D(R-H) reported by Weissman and Benson. (37)
While the first three members seem to vary approximately in accordance with the Evans-Polanyi relation (E-P) the reaction OH + $CHCl_3$ has a remarkably high activation energy which is completely out of line with the other reactants.
Thus, both of the Arrhenius parameters (A, E_a) vary in a very irregular manner through the series of Cl-substituted methanes. The case of $CHCl_3$ clearly demonstrates that the C-H bond energy is not the sole factor in controlling the activation energy.
Jeong and Kaufman (25) have studied the same series of reactions and they calculated theoretical values of the A-factors based on estimated transition state entropies using a method developed by Benson. (38) They find that the theoretical A-factors deviate strongly from the experimental values in certain cases (e.g. $CHCl_3$ and CH_2Cl_2) and it was not possible to indicate a physical explanation for these discrepancies within the framework of current transition state theories.
At present there is a rapid development within the theories of reactive collisions based on the very detailed information that can be obtained in molecular beam experiments. It is expected that a rigorous theory will emerge which allows the chemist to calculate reliable Arrhenius parameters from "first principles" i.e. from a relatively small set of molecular parameters which govern the kinematics (e.g. distance of closest

approach) and the integrated reaction probability during the collision.

So far, however, theoretical predictions cannot replace experimental studies on the rate constants of elementary gas phase reactions. In view of the strong acute demand for reliable rate constants as input for atmospheric chemistry modelling it is very encouraging that the different experimental techniques developed in recent years appear to give essentially the same results.

11.3 Tropospheric lifetimes

The reaction with OH is the principal removal process for natural trace constituents of the atmosphere like CH_4 and CH_3Cl which are present in mole fractions of 1.7×10^{-6} and 6.5×10^{-10}, respectively. The chemical half-life of a particular species "S" is governed by the rate constant, $k_S = k(OH+S)$ and the steady state concentration of hydroxyl radicals, $t(1/2)_S = \ln 2 / k_S (OH)_{SS}$. The effect of the sink reaction is to reduce the concentration of S below the value determined by diffusion alone. Thus, in the stratosphere at 30-km altitude the CH_4 mole fraction is reduced to half of its tropospheric value while that of CH_3Cl is down by a factor of twenty. This difference in concentration ratios reflects the difference in the rate constants, $k(OH+CH_3Cl) > k(OH+CH_4)$. For the antropogenic chloro-fluoro-carbons (CFC) OH also serves as a sink that prevents or reduces their transport into the stratosphere where they would add to the pool of catalytic ozone removal reactions. Therefore, the unreactive CFC-12 and

slowly reacting compounds such as CFC-22 should preferently be replaced by more reactive compounds like CH_2Cl_2 in future technological applications. It would seem far better, of course, if halogen-free compounds could replace the CFC´s in cases involving unavoidable and large release rates.

11.4 Future work

The major part of the present experimental work was quite successful. However, our experimental results on the reactions $CH_4+OH \rightarrow CH_3+H_2O$ and $CH_3CCl_3+OH \rightarrow CH_2CCl_3+H_2O$ were abandoned because of small amounts of highly reactive impurities present in the applied reactant samples. These reactions, as well as the reaction $OH+CHCl_3 \rightarrow H_2O+CCl_3$, will have to be re-investigated under improved experimental conditions, i.e. using high-purity gases and taking into account certain constraints on concentration ratios, $p(RH)/p(H_2O)$, which were found to be critical in our computer simulations.

In our experimental work on $OH + CHCl_3 \rightarrow H_2O + CCl_3$ we recorded an ultraviolet absorption spectrum which we tentatively assigned to the CCl_3-radical. We intend to investigate the kinetics of CCl_3 in the presence of O_2 where the following reactions may occur:

(1) $CCl_3 + O_2 \rightarrow CCl_3O_2$

(2) $CCl_3O_2 \rightarrow COCl_2 + ClO$ (?)

(3) $2\ CCl_3O_2 \rightarrow 2\ CCl_3O + O_2$

(4) $CCl_3O \rightarrow COCl_2 + Cl$ (?)

(5) $2\ CCl_3O \rightarrow 2\ COCL_2 + Cl_2$

The adduct CCl_3O_2 formed in reaction (1) is expected to absorb light in the UV-region (around 2500 Å) and if this is true we may be able to study the subsequent reactions which may be any of the hypothetical reactions (2) - (5). Phosgene ($COCl_2$) is a probable stable product which may hydrolyze and "rain out" under atmospheric conditions. CCl_3 may serve as a prototype of the radicals derived from the various CFC's (chloro-fluoro-carbons) and the ultimate fate of these radicals are of prime interest to the current debate on ozone depletion. At present very little is known about the oxidation of Cl- and F-substituted hydrocarbons, but it is assumed that the oxidation has a pathway similar to that of CH_3.

Our experiments on $CCl_3 + O_2$ may help to identify the more important reaction channels and eventually clear up the complete reaction mechanism.

Acknowledgements.

We wish to thank our collegues at the Chemistry Department for many helpful and stimulating discussions on various aspects of gas phase kinetics, thermochemistry and analytical chemistry. In experiments on reactant molecules like CH_4 which reacts rather slowly with OH competition with highly reactive impurities becomes a serious problem. Therefore we are most grateful to Helge Egsgaard for his careful GC/MS analysis of our most critical gas samples. In our analysis of the experimental results we have been heavily supported by the Computer Department. The treatment of more than 500 kinetic curves is quite a formidable task which was greatly facilitated by a fast-access interactive computer program with graphics display which was developed by Steen Madsen. Our most important analytical tool is an advanced computer program for simulation of chemical kinetics by Ole Lang Rasmussen. This program allows a rigorous test of any proposed reaction mechanism because the response of the model to variations in selected parameters can be directly compared with the experimental results by superposition of model curves on experimental decay curves displayed on a graphical terminal.

Last, but not least, we are in in debt to K.B. Hansen and his co-workers at the Electronics Department. The successful development of the state-of-the-art pulse radiolysis instrumentation for studies of gas phase kinetics is the result of the collaboration of highhly qualified experts on electronics, optical spectroscopy and mini-computers. The excellent quality

(S/N-ratio) of our experimental decay curves is largely due to the Xe-lamp pulsing devise developed by Thorkild Hviid. The optical feed-back system developed at a later stage improved the long-term stability and provided reproducible light pulses with a constant light intersity over 5-10 msec which is necessary in studies of slowly decaying transient species.
We are still using an old PDP-8 mini-computer with a fairly limited storage capacity. Nevertheless, thanks to Jens V. Olsen we were supplied with a high efficiency software package providing all of the options necessary for data-transfer, function conversions, pre-view graphics and file manipulation. The over-all performance of the complete system is excellent including the long-term stability. We are grateful to the Electronics Service Division for maintaining the set-up in superb condition. In the daily routine work we have enjoyed the collaboration with Preben Lauge Genske who runs the Febetron 705 B accelerator and keeps it operational with fine puls-to-pulse reproducibility. Obviously, without the co-operation of all of these collegues and good friends we could have accomplished very little and we think it is appropriate to point out that our success rests upon their continued support.

References

(1) M.J. Molina and F.S. Rowland, Nature, 249,810 (1974)

(2) UNEP, Bulletin No.7 (Assessment of Ozone Layer)
January 1982

(3) National Academy of Science report 1982
"Causes and Effects of Stratospheric Ozone Reduction"
An Update.

(4) D.L. Baulch, R.A. Cox, P.J. Crutzen, R.F. Hampson Jr.,
J.A. Kerr, J. Troe and R.T. Watson. (CODATA Task Group)
J. Phys. Ref.Data, 11,327 (1982)

(5) R. Atkinson,
Advances in Photochemistry, 11,404 (1979)

(6) M.C. Sauer
Advances in Radiation Chemistry

(7) R.S. Dixon
Radiation Research Reviews 2,237 (1970)

(8) S. Gordon and W.A. Mulac
International Journal of Chemical Kinetics
Symposium No.1, 1975. Proceedings p.289

(9) A.W. Boyd, C. Willis, and O.A. Miller
Can. J. Chem. 51,4048 (1973)

(10) G.H. Dieke and H.M. Crosswhite
Report No. 87 (Bumblebee Series)
The Johns Hopkins University, Baltimore, Maryland.

(11) Elaine A. Moore and W.G. Richards
Physica Scripta 3,223 (1971)

(12) V. Kondratjew
Acta Physiochem. U.S.S.R. 8,315 (1938)

(13a) O. Oldenberg and F.F. Rieke
J. Chem. Phys. 7,485 (1939)

(13b) A.A. Frost, O. Oldenberg
J.Chem.Phys. 4, 642 (1936)

(14) P. Fowler, M.de Sorgo, A.J. Yarwood, O.P. Stowersy, H.E. Gunning J. Amer. Chem. Soc., 89,1352 (1957)

(15) A.B. Callear and W.J. Tyerman
Trans. Faraday Soc., 62,371 (1966)

(16) S. Gordon, W.A. Mulac and P. Nangia
J. Phys. Chem., 75,2087 (1971)

(17) J.U. White
J. Opt. Soc. Am., 32,285 (1942)

(18) C. Willis and A.W. Boyd
Int. J. Radiat. Phys. Chem., 8,71 (1976)

(19) E.C.Y. Inn and Y. Tanaka
J. Opt. Soc. Am., 43, 870 (1953)

(20) O. Lang Rasmussen
Risø Report No. 395 (1979)

(21a) P.B. Pagsberg, J. Eriksen and H.C. Christensen
J. Phys. Chem. 83,582 (1979)

(21b) C. Willis and A.W. Boyd
Int.J.Radiat.Phys.Chem., 8, 71 (1976)

(22) N.R. Greiner
J.Chem.Phys., 53, 1070 (1970)

(23a) R.P. Overend, G. Paraskevopoulus and R.J. Cvetanovic
Can.J.Chem., 53, 3374 (1975)

(23b) C.J. Howard and K.M. Evenson
J.Chem.Phys., 64, 4303 (1976)

(24) G. Black and G. Porter
Proc.Roy.Soc. London A 266, 185 (1962)

(25) K. Jeong and Kaufman
J.Phys.Chem., 86, 1808-21 (1982)

(26) D.D. Davis, G. Machado, B. Conaway, Y. Oh and R.T. Watson
J.Chem.Phys., 65, 1268 (1976)

(27) R.A. Perry, R. Atkinson and J.N. Pitts, Jr.
J.Chem.Phys., 64, 1618 (1976)

(28) C.J. Howard and K.M. Evenson
J.Chem.Phys., 64, 197 (1976)

(29) R. Atkinson, D.A. Hansen and J.N. Pitts, Jr.
J.Chem.Phys., 63, 1703 (1975)

(30) R.T. Watson, G. Machado, B. Conoway, S. Wagner and
D.D. Davis J.Phys.Chem., 81, 256 (1977)

(31) J.-S. Chang and F. Kaufman
J.Chem.Phys., 66, 4989 (1977)

(32) V. Handwerk and R. Zellner
Berichte Bunsen Ges.Phys.Chem., 82, 1161 (1979)

(33) M.A.A. Clyne and P.M. Holt
J.Chem.Soc., Faraday Trans 2, 75, 582 (1979)

(34) G. Paraskevopouloz, D.L. Singleton and R.S. Irvin
J.Phys.Chem., 85, 561 (1981)

(35) I.M.Campbell, D.F. McLaughlin and B.J. Handy
Chem.Phys.Lett., 38, 362 (1976)

(36) M.G. Evans and M. Polanyi
Trans. Faraday Soc. 34, 11 (1938)

(37) Maia Weissman and S.W. Benson
J. Phys. Chem. 87, 243 (1983)

(38) S.W. Benson
"Thermochemical Kinetics", 2nd ed., Wiley, New York (1976)

Fig.6.1

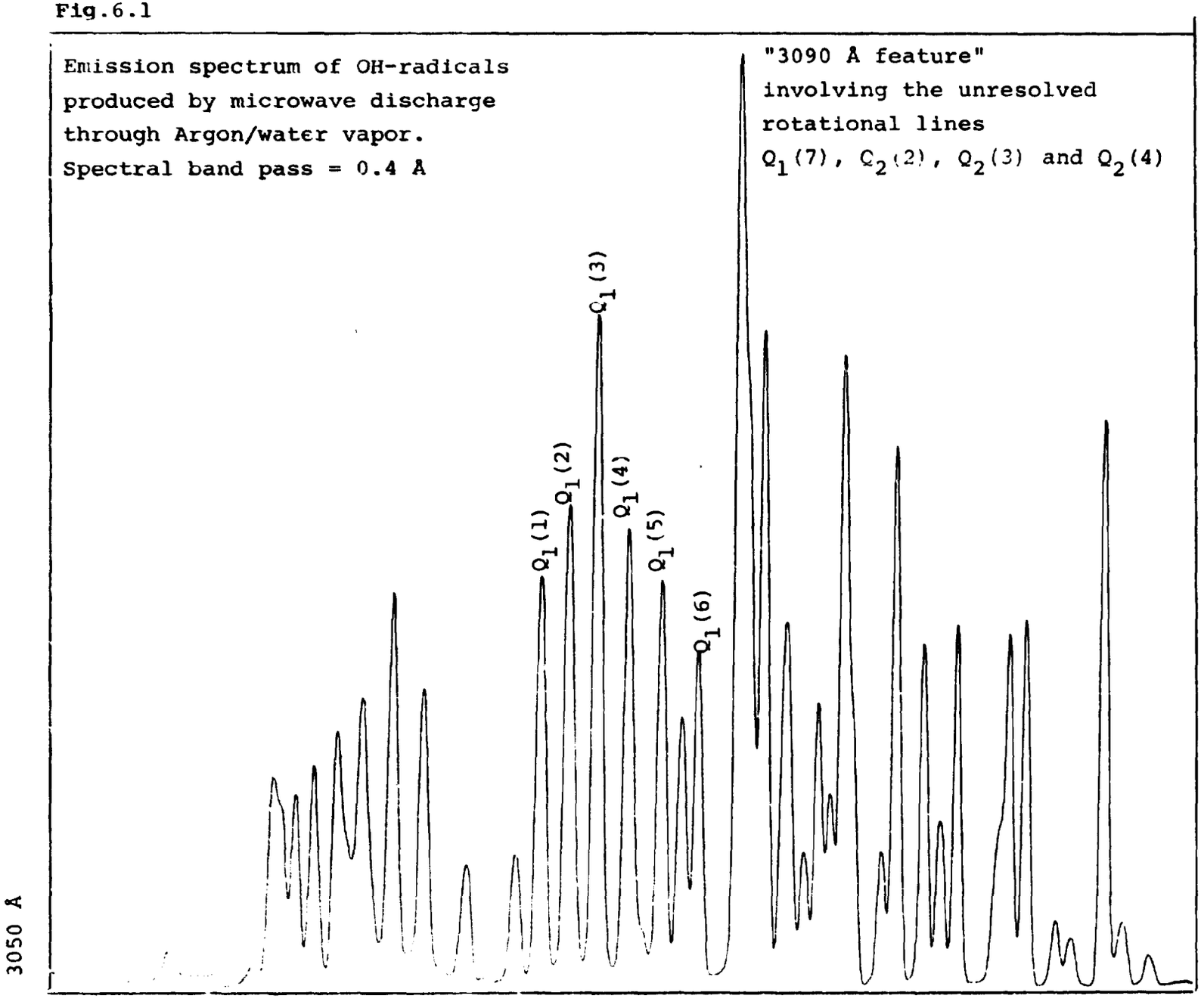
Emission spectrum of OH-radicals
produced by microwave discharge
through Argon/water vapor.
Spectral band pass = 0.4 Å
"3090 Å feature"
involving the unresolved
rotational lines
$Q_1(7)$, $Q_2(2)$, $Q_2(3)$ and $Q_2(4)$
$Q_1(1)$
$Q_1(2)$
$Q_1(3)$
$Q_1(4)$
$Q_1(5)$
$Q_1(6)$
3050 Å
3130 Å

Fig. 7.1

"Natural decay" of hydroxyl radicals via the combination reactions

$OH + OH = H_2O_2$ $OH + OH = H_2O + O$ and $OH + H = H_2O$

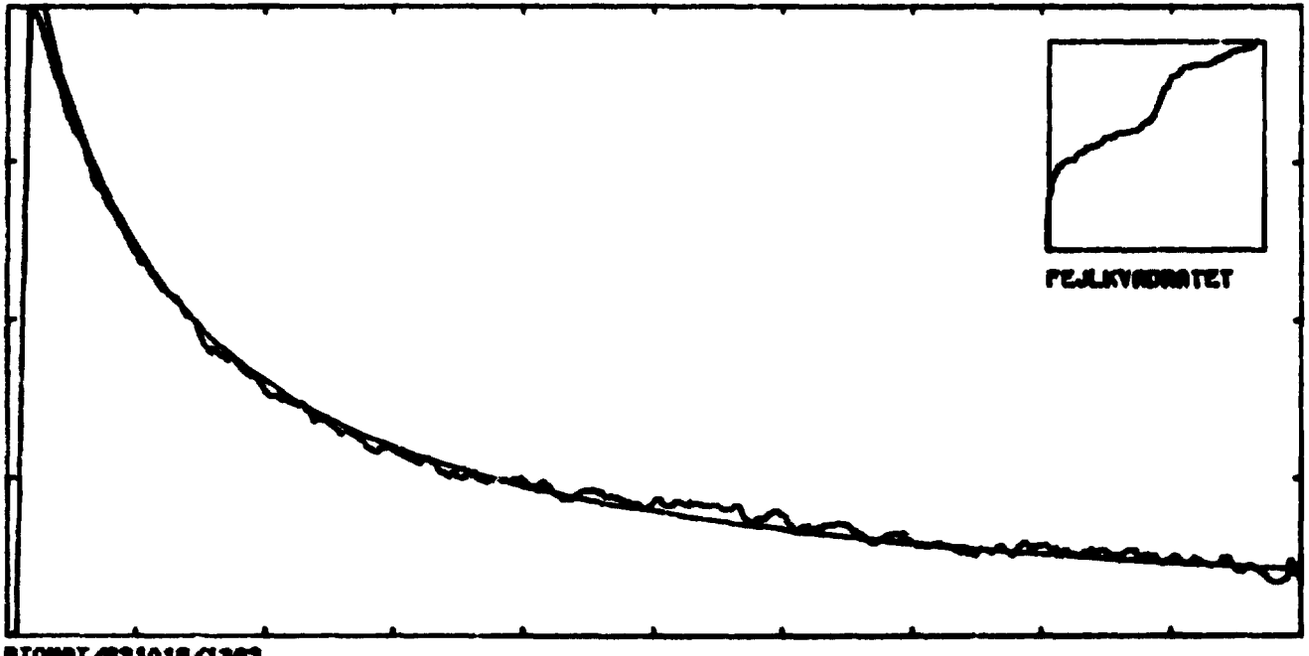

Fig. 7.2

Exponential decay of OH controlled by the reaction

$$OH + C_2H_6 = H_2O + C_2H_5$$

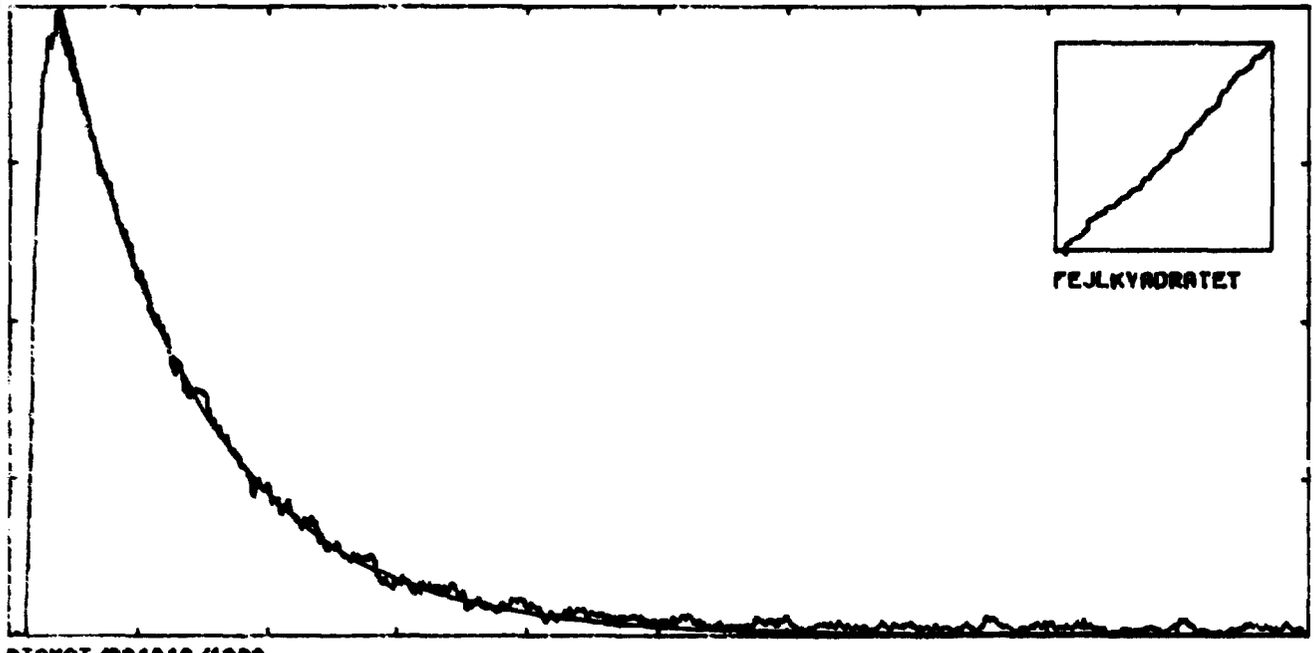

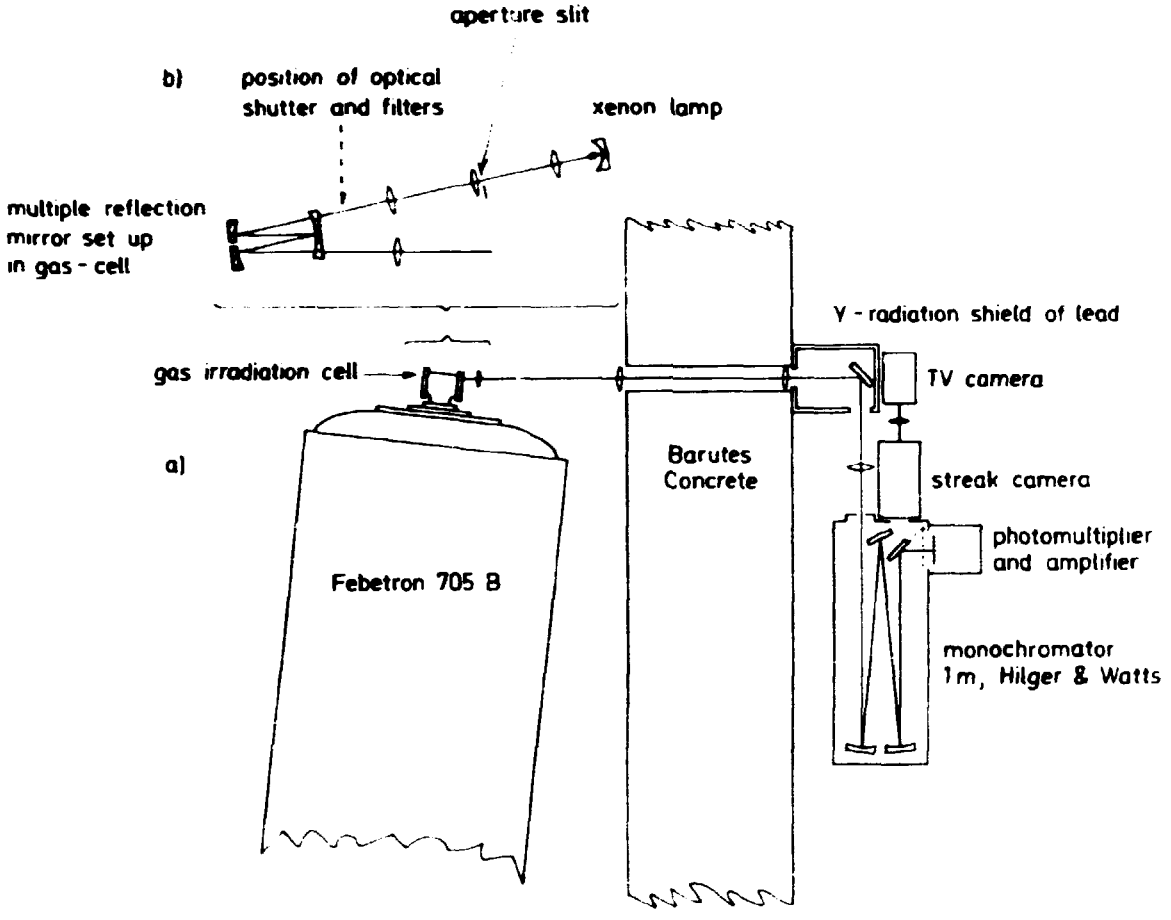

Fig.8.1 Schematic diagram of the experimental gas phase pulse-radiolysis set-up. a) lay-out in horizontal plane. b) enlarged vertical cut showing the optics handling the analyzing light beam from the xenon lamp light source and through the irradiation cell. More details shown in Fig.8.2.

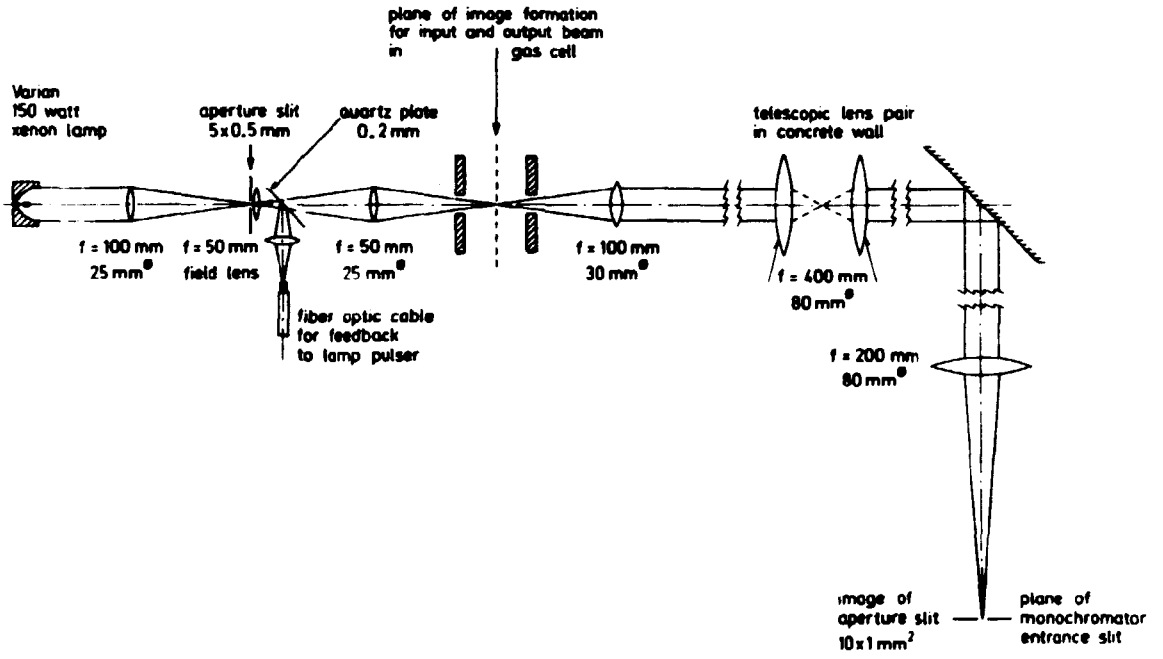

Fig.8.2 The basic components of the pulse-radiolysis optical system. For the sake of simplicity, the set of conjugate mirrors in the irradiation cell has been omitted by letting the planes of image formation for imput and output beams in the irradiation cell coincide. Beam shapes are shown in a plane orthogonal to aperture and monochromator slits.

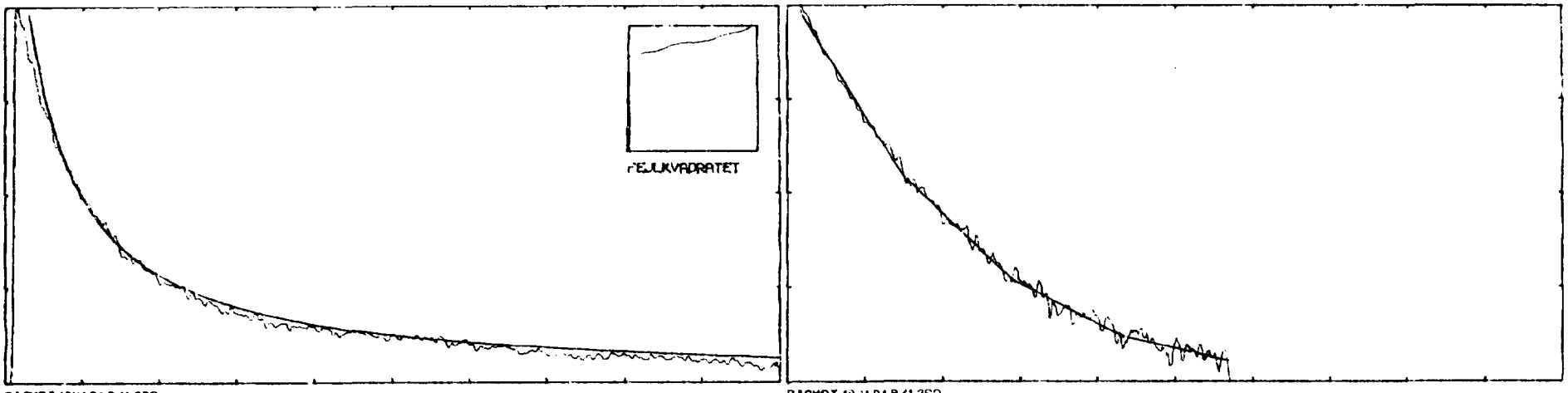

Fig. A 10.1

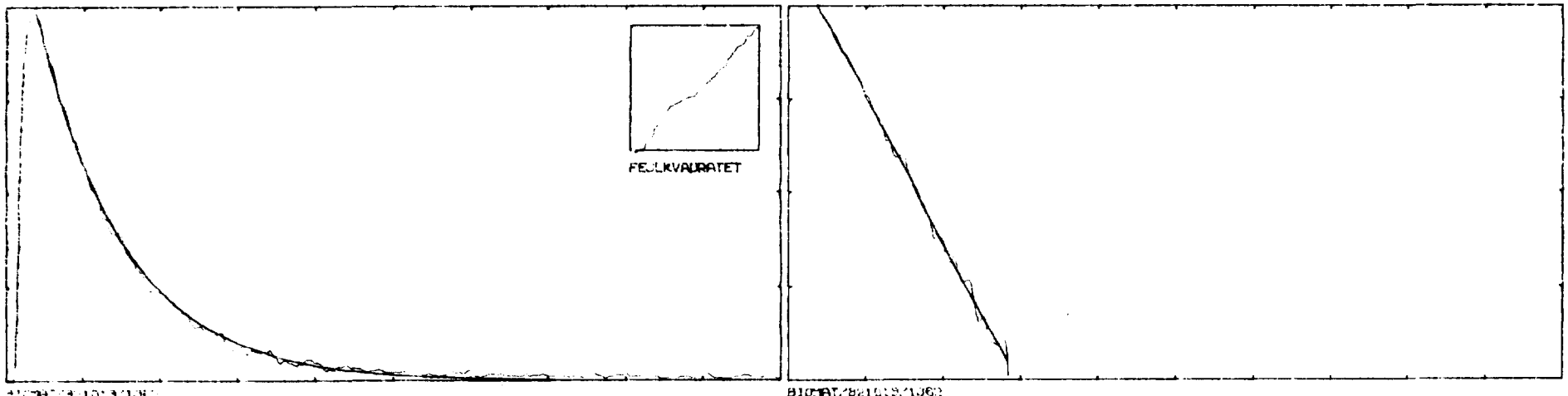

PLOT NO. 02, EFF: 61%, PLOTTIME: 310 SECS.

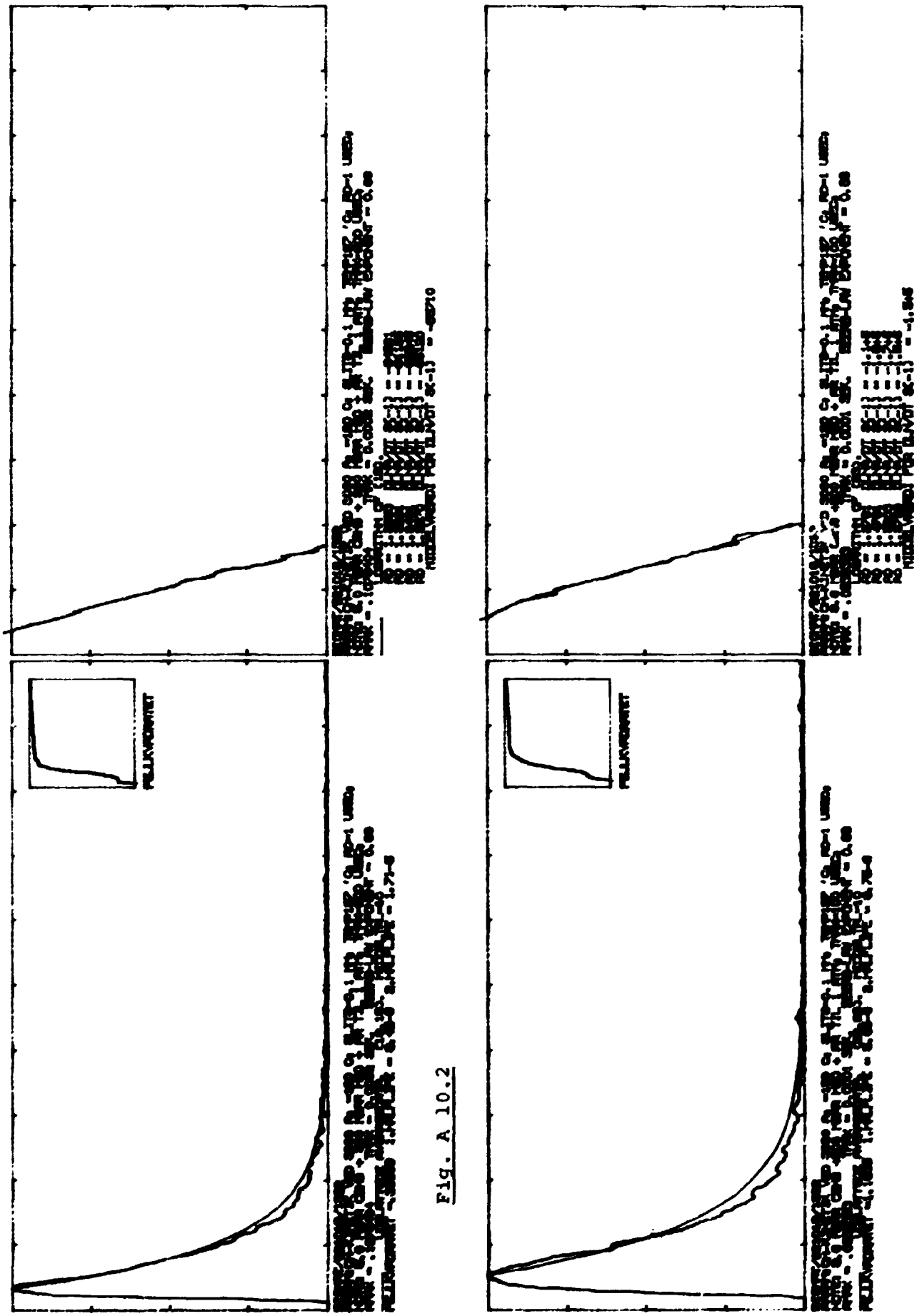

Fig. A 10.2

Fig. A 10.3

LEFT: Reciprocal half-life of OH versus the concentration of C_2H_6

RIGHT: dln(OH)/dt versus the concentration of C_2H_6

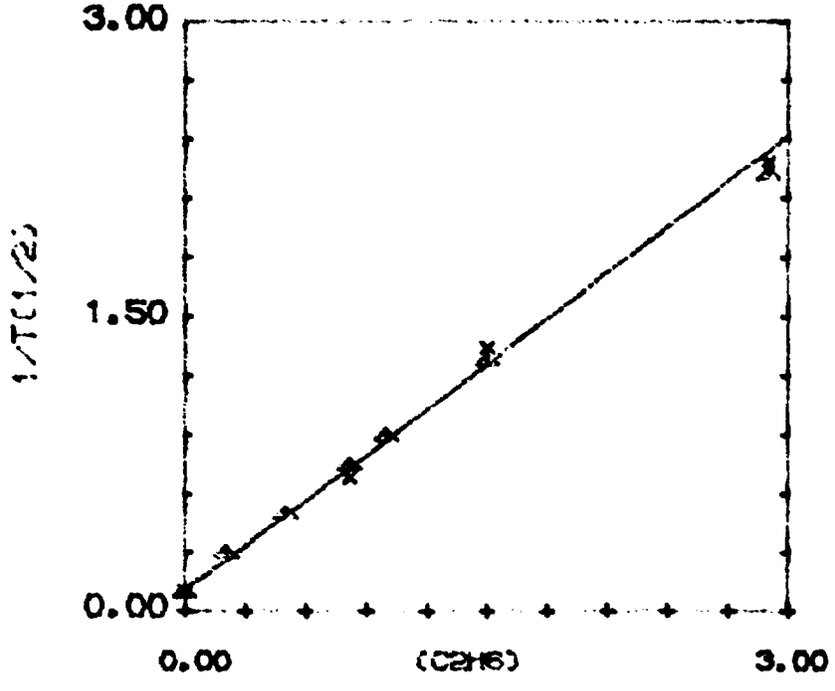

DATE: 21 1 83 RUN: 3

PROGRAM PLOTOPTIONS

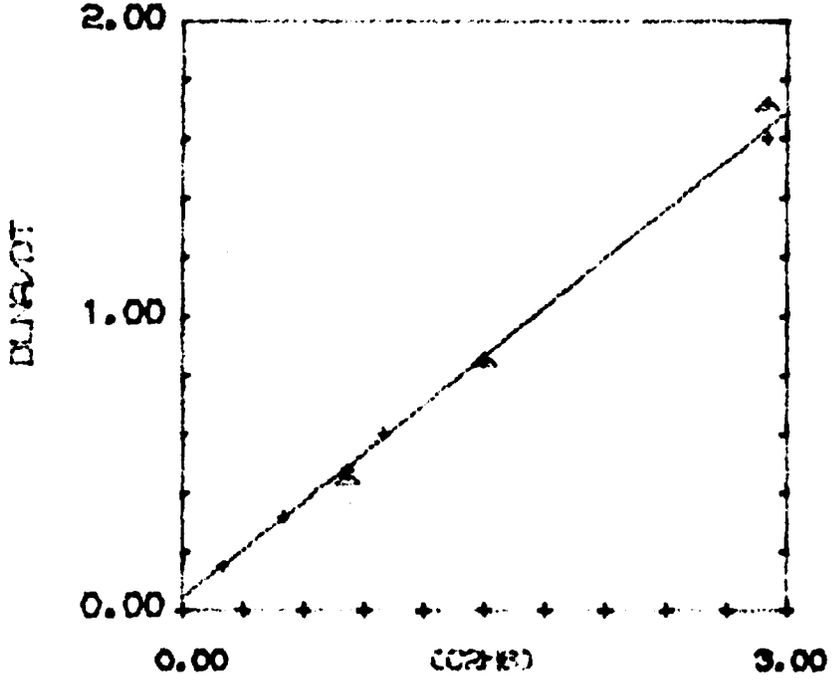

DATE: 21 1 83 RUN: 3

PROGRAM PLOTOPTIONS

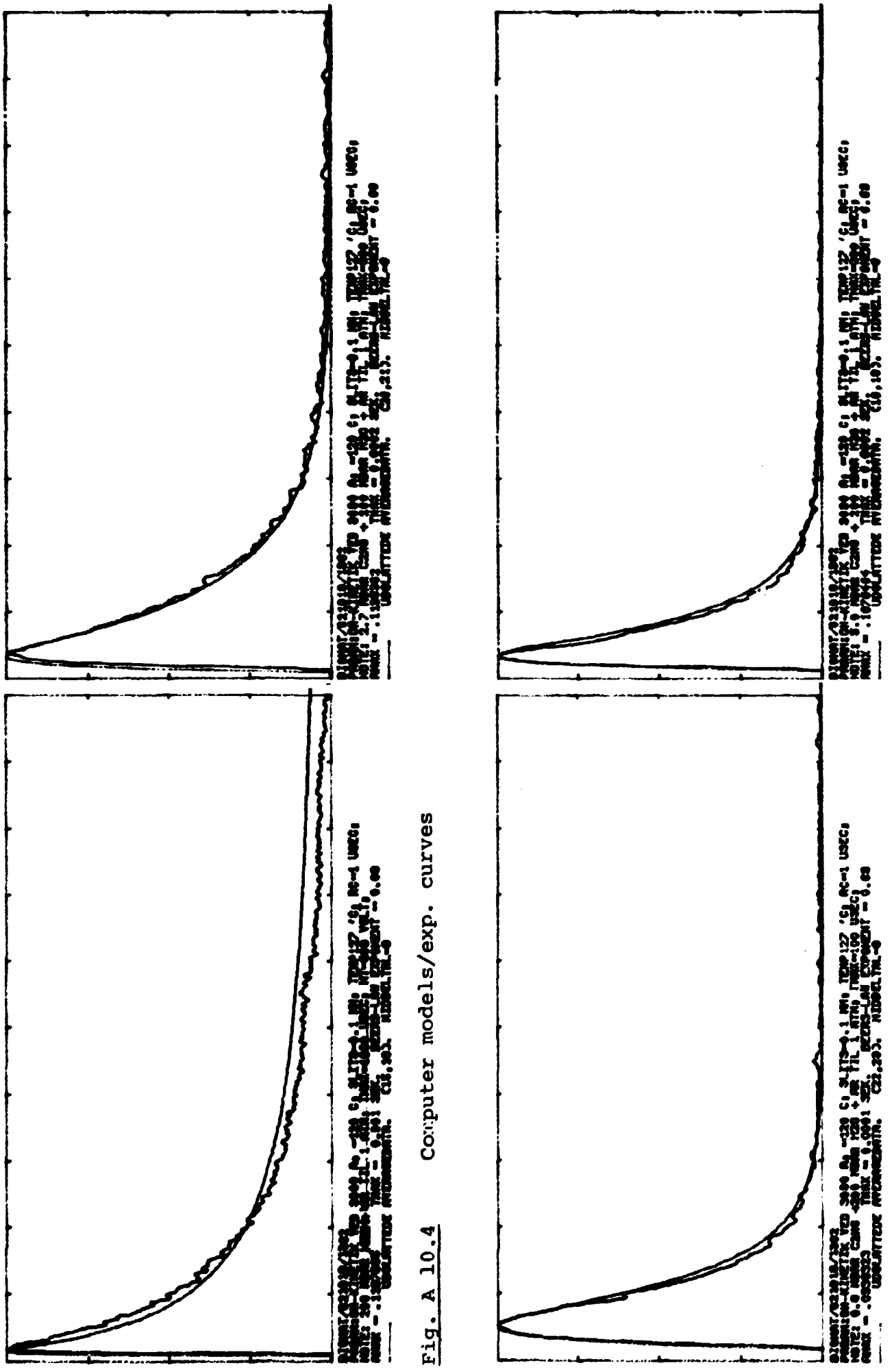

Fig. A 10.4 Computer models/exp. curves

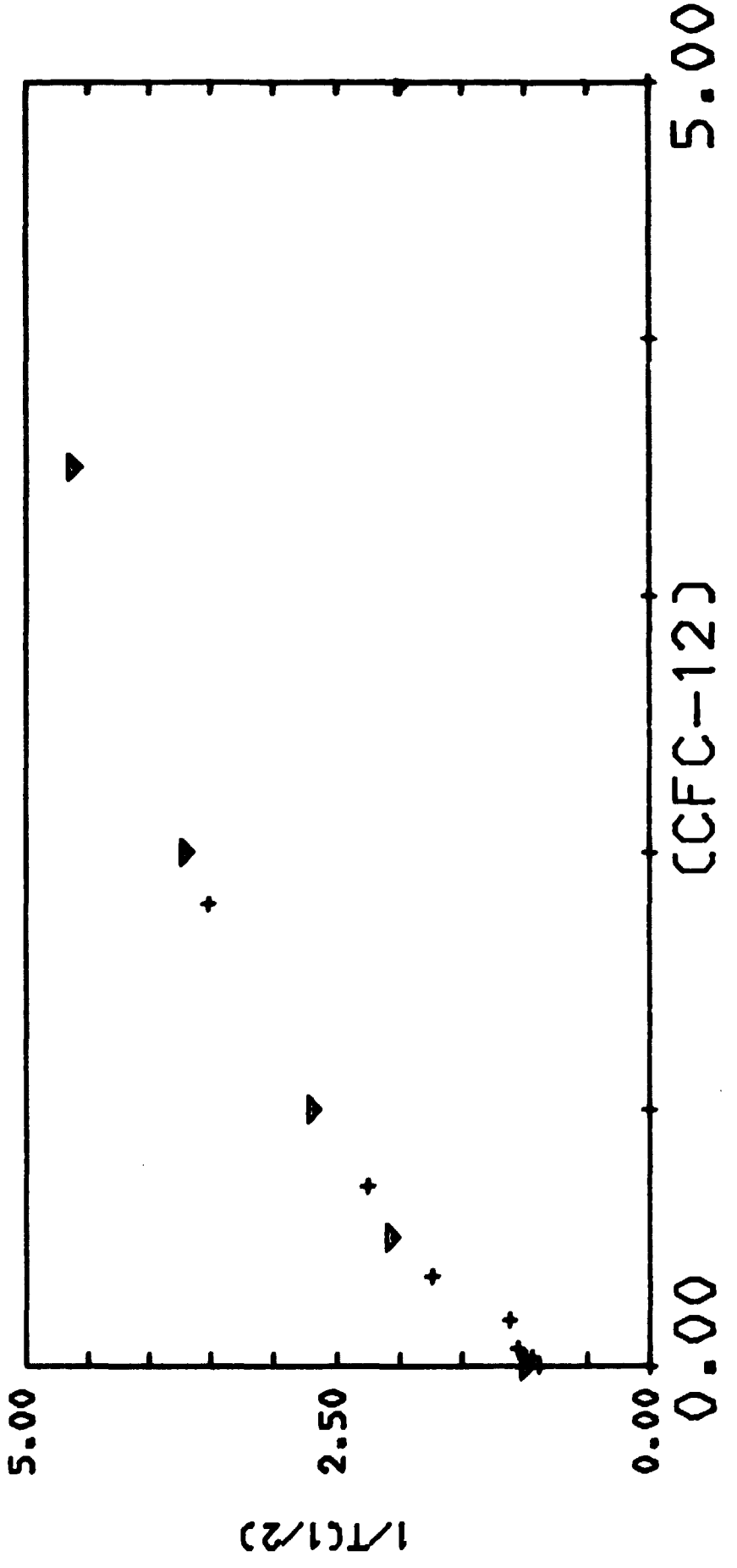
5.00
2.50
0.00
0.00
5.00
1/T(1/2)
(CFC-12)
OH/CFC-12
PROGRAM PLOTOPTIONS
DATE: 14 4 1983 RUN: 1

Fig. A 10.5

Fig. A 10.6

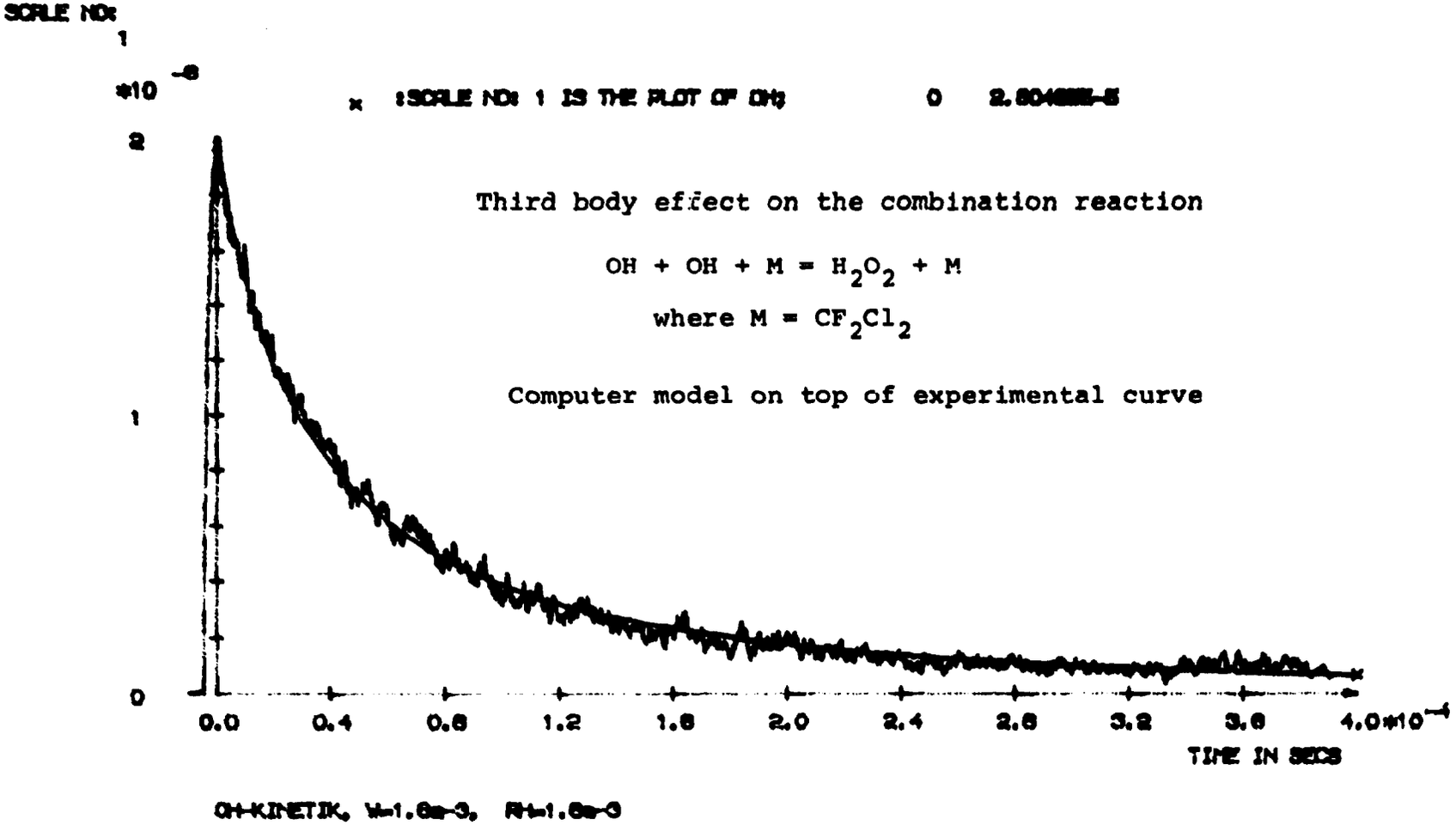

Third body effect on the combination reaction

$$OH + OH + M = H_2O_2 + M$$

where $M = CF_2Cl_2$

Computer model on top of experimental curve

A 10.1

$C_2H_6 + OH = C_2H_6 + H_2O$; t = 27°C Biomat/821012/9015.

run nr	$p(C_2H_6)$	(C_2H_6)	τ	dlA/dt	A_{max}
31,32	0	0	100.0		0.129
33,34	3.5×10^{-3}	1.42×10^{-4}	23.1	2.89×10^{4}	0.092
35,36	7.2	2.93	12.2	5.66	0.082
37,38	10.4×10^{-2}	4.23	7.4	8.36	0.069
	Atm.	mol/l	μ sec	sec^{-1}	

$\tau = \tau(1/4) - \tau(1/2)$ when $p(C_2H_6) > 0$

$\tau = \tau(1/4) - \tau(1/2)/2$ when $p(C_2H_6) = 0$

$k(I) = 1.69 \times 10^8\ m^{-1}s^{-1}$

$k(II) = 1.95 \times 10^8\ m^{-1}s^{-1}$

A 10.1

$C_2H_6 + OH = C_2H_5 + H_2O$; t = 48°C Biomat/821013/2274.

run nr	$p(C_2H_6)$	(C_2H_6)	τ	dlnA/dt	A_{max}
16,17	0	0	84.7		0.129
18,19	0	0	96.5		0.119
20,21	0	0	107.6		0.121
23,24	1.1×10^{-3}	4.2×10^{-5}	56.6	1.48×10^{4}	0.098
25,26	1.1	4.2	44.4	1.67	0.117
27,28	2.1	8.0	26.8	2.53	0.115
29	5.0	1.9×10^{-4}	12.3	5.76	0.099
30,31	5.0	1.9	13.3	5.38	0.075
34,35	1.0×10^{-2}	3.8	5.7	1.27×10^{5}	0.098
36	1.0	3.8	5.3	1.23	0.097
	Atm.	mol/l	μ sec	sec^{-1}	

$\tau=\tau(1/4)-\tau(1/2)$ when $p(C_2H_6)>0$

$\tau=\tau(1/4)-\tau(1/2)/2$ when $p(C_2H_6)=0$

$k(I)=2.46\times10^{8}\ m^{-1}s^{-1}$

$K(II)=2.58\times10^{8}\ m^{-1}s^{-1}$

A 10.1

$C_2H_6 + OH = C_2H_5 + H_2O$; t = 100°C Biomat/821014/5242.

run nr	$p(C_2H_6)$	(C_2H_6)	τ	dlnA/dt	A_{max}
27,28	0	0	56.2		0.112
29	0	0	41.5		0.125
30,31	2.3×10^{-3}	7.6×10^{-5}	19.4	3.45×10^{4}	0.090
32,33	2.3	7.6	18.2	4.23	0.107
34	5.3	1.8×10^{-4}	6.8	9.01	0.097
35,36	5.3	1.8	8.9	8.46	0.100
37,38	1.1×10^{-2}	3.5	4.7	1.45×10^{5}	0.106
	Atm.	mol/l	μ sec	sec^{-1}	

$\tau=\tau(1/4)-\tau(1/2)$ when $p(C_2H_6)>0$

$\tau=\tau(1/4)-\tau(1/2)/2$ when $p(C_2H_6)=0$

$k(I)=3.70\times10^{8}\ m^{-1}s^{-1}$

$k(II)=3.94\times10^{8}\ m^{-1}s^{-1}$

A 10.1

$C_2H_6 + OH = C_2H_6 + H_2O$; t = 127°C Biomat/821018/1362.

run nr	$p(C_2H_6)$	(C_2H_6)	τ	dlnA/dt	A_{max}
15,16	0	0	67.3		0.119
17	5.0×10^{-3}	1.5×10^{-4}	7.7	8.37×10^{4}	0.107
20,21	2.7	8.2×10^{-5}	10.1	4.37	0.114
22,23	9.6	2.9×10^{-4}	4.1	1.60×10^{5}	0.094
	Atm.	mol/l	μ sec	sec^{-1}	

$\tau = \tau(1/4) - \tau(1/2)$ when $p(C_2H_6) > 0$

$\tau = \tau(1/4) - \tau(1/2)/2$ when $p(C_2H_6) = 0$

$k(I) = 5.30 \times 10^{8}\ m^{-1}s^{-1}$

$k(II) = 5.40 \times 10^{8}\ m^{-1}s^{-1}$

A 10.2

F-12 + OH; t = 27°C Biomat/821011/5029.

run nr	p(F-12)	(F-12)	τ	dlnA/dt	A_{max}
45,46	3.4×10^{-2}	1.4×10^{-4}	95.6		0.114
47,48	7.5	3.1	73.2		0.106
49,50	1.0×10^{-2}	4.1	66.7		0.118
51	1.5	6.1	38.4		0.105
	Atm.	mol/l	μ sec	sec^{-1}	

A 10.2

P-12 + OH; t = 75°C Biomat/820928/0530.

run nr	p(P-12)	(P-12)	τ	dlnA/dt	A_{max}
10,11,12	0	0	75.2		0.118
13	1.0×10^{-3}	3.5×10^{-5}	100.0		0.121
14,15,16	1.0	3.5	106.0		0.118
17,18,19	2.0	7.0	94.4		0.112
20,21,22	5.0	1.8×10^{-4}	88.9		0.110
23,24,26	1.0×10^{-2}	3.5	57.5		0.101
27	2.0	7.0	44.4		0.092
28,29	2.0	7.0	39.6		0.100
30,32,33	5.0	1.8×10^{-3}	28.4		0.085
34,35	0	0	112.0		0.120
	Atm.	mol/l	μ sec	sec^{-1}	

A 10.3

$CH_4 + OH = CH_3 + H_2O$; t = 27°C Biomat/821011/5029.

run nr	p(CH_4)	(CH_4)	τ	dlnA/dt	A_{max}
1	0	0	64.0		0.133
6,7	0	0	122.0		0.114
9	0	0	129.0		0.116
11	0	0	125.0		0.121
12,13	1.0×10^{-2}	4.2×10^{-4}	89.0	1.15×10^{4}	0.090
14,15	1.0	4.2	84.4	1.22	0.089
16,17	1.0	4.2	78.9	1.24	0.098
18,19	1.5	6.2	55.6	1.97	0.091
20,21	2.0	8.0×10^{-3}	32.2	3.05	0.077
22,23	2.5	1.0	40.0	3.00	0.081
26,27	3.3	1.3	42.2	2.23	0.075
29	3.3	1.3	37.8	3.14	0.098
30,31	0	0	90.0		0.132
32	0	0	96.0		0.118
33	0	0	98.0		0.119
43	0	0	72.2		0.135
44	0	0	72.6		0.125
	Atm.	mol/l	μ sec	sec^{-1}	

A 10.3

$CH_4 + OH = CH_3 + H_2O$; t = 48°C Biomat/821013/2274.

run nr	p(CH_4)	(CH_4)	τ	dlnA/dt	A_{max}
2	0	0	68.0		0.082
3,4	0	0	81.0		0.103
5	0	0	79.0		0.105
6	0	0	79.0		0.109
7,8	7.5×10^{-3}	2.9×10^{-4}	54.0	7.15×10^{3}	0.104
9	1.3×10^{-2}	4.79	60.0	6.49	0.092
10,11	2.1	7.9	39.5	1.66×10^{4}	0.086
12,13	3.2	1.2×10^{-3}	29.5	2.48	0.089
14,15	4.1	1.6	24.0	3.19	0.086
	Atm.	mol/l	μ sec	sec^{-1}	

A 10.3

$CH_4 + OH = CH_3 + H_2O$; t = 72°C Biomat/821001/8778.

run nr	$p(CH_4)$	(CH_4)	τ	$d\ln A/dt$	A_{max}
21,22	2.0×10^{-2}	7.06×10^{-4}	28.9	2.12×10^{4}	0.104
23,24	5.0	1.77×10^{-3}	23.8	2.84	0.102
25,26	10.0	3.53	7.4	9.62	0.061
	Atm.	mol/l	μ sec	sec^{-1}	

A 10.3

$CH_4 + OH = CH_3 + H_2O$; t = 75°C Biomat/821007/0442.

run nr	$p(CH_4)$	(CH_4)	τ	dlnA/dt	A_{max}
1	0	0	60.7		0.129
2	0	0	76.7		0.108
3	0	0	73.3		0.110
4	0	0	65.6		0.117
9,10	0	0	83.0		0.132
11,12	0	0	80.0		0.129
13,14	5.7×10^{-3}	2.0×10^{-4}	58.0	7.40×10^{3}	0.114
15,16	1.0×10^{-2}	3.54	48.0	1.12×10^{4}	0.111
17,18	2.2	7.6	29.0	2.05	0.112
19,20	4.1	1.4×10^{-3}	16.9	3.62	0.102
22	8.3	2.9	7.5	7.63	0.073
21,23,24	8.3	2.9	9.3	6.66	0.082
25,26,27	10.6	3.7	10.0	1.40×10^{5}	0.080
29,30	0	0	79.0		0.125
	Atm.	mol/l	μ sec	sec^{-1}	

A 10.3

$CH_4 + OH = CH_3 + H_2O$; t = 100°C Biomat/821011/4105

run no	$p(CH_4)$	(CH_4)	τ	dlnA/dt	A_{max}
6,7	0	0	75.0		0.122
8,9	1.05×10^{2}	3.43×10^{-4}	40.0	1.66×10^{4}	0.107
10,11	2.00	6.54	24.7	2.84×10^{4}	0.137
12,13	4.50	1.47×10^{-3}	16.2	4.71×10^{4}	0.109
14	9.04	2.96	8.1	9.00×10^{4}	0.182
16,17	9.04	2.96	8.4	8.46×10^{4}	0.096
18,19	0	0	65.0		0.121
	Atm.	mol/l	μ sec	sec^{-1}	

A 10.3

$CH_4 + OH = CH_3 + H_2O$; t = 100°C Biomat/821014/5242.

run nr	$p(CH_4)$	(CH_4)	τ	dlnA/dt	A_{max}
2,3	0	0	86.1		0.124
4,5	5.4×10^{-3}	1.8×10^{-4}	67.0	6.67×10^{3}	0.099
6,7	1.1×10^{-2}	3.5	45.5	1.15×10^{4}	0.105
8,9	1.9	6.1	28.6	2.28	0.108
10,11	2.6	8.5	20.4	3.14	0.100
12,13	3.5	1.2×10^{-3}	18.4	3.60	0.091
14,15	7.2	2.4	8.3	7.94	0.089
	Atm.	mol/l	μ sec	sec^{-1}	

A 10.3

$CH_4 + OH = CH_3 + H_2O$; t = 127°C Biomat/821018/1362.

run nr	$p(CH_4)$	(CH_4)	τ	dlnA/dt	A_{max}
9	0	0	85.6		0.117
2	0	0	94.4		0.120
3,4	9.8×10^{-3}	3.0×10^{-4}	43.0	1.46×10^{4}	0.118
5.6	9.8	3.0	46.7	1.57	0.111
7,8	2.0×10^{-2}	6.1	33.3	2.53	0.116
9,10	5.5	1.7×10^{-3}	12.8	5.76	0.103
11,12	5.5	1.7	10.6	7.03	0.094
	Atm.	mol/l	μ sec	sec^{-1}	

A 10.4

$CH_3Cl + OH = CH_2Cl + H_2O$; t = 27°C Biomat/821011/5029.

run nr	$p(CH_3Cl)$	(CH_3Cl)	τ	dlnA/dt	A_{max}
71,72	0	0	137.8		0.133
73,74	0	0	152.0		0.117
75	7.5×10^{-3}	3.1×10^{-4}	29.0	2.30×10^{4}	0.067
76,77	7.5	3.1	19.2	2.52	0.090
78,79	1.5×10^{-2}	6.2	10.6	5.76	0.069
80	2.3	9.28	5.6	6.77	0.057
81,82	2.3	9.28	9.1	7.20	0.041
83,84	2.0	8.1	7.7	7.43	0.056
85,86	0	0	200.0		0.112
	Atm.	mol/l	μ sec	sec^{-1}	

$k(I) = 1.03\times10^{8}$

$k(II) = 8.7\times10^{7}$

A 10.4

SF_6 + OH; t = 50°C Biomat/820923/1003.

run nr	p(SF_6)	(SF_6)	τ	dlnA/dt	A_{max}
13,14	0	0	119.4		0.116
15,16	0	0	122.2		0.114
17,18	1.0×10^{-3}	3.7×10^{-5}	116.7		0.114
19,20	2.0	7.5	105.6		0.112
21,22	4.0	1.5×10^{-4}	94.4		0.114
23,24	1.0×10^{-2}	3.76	100.0		0.120
27,28	0	0	77.8		0.121
29,30	1.0	3.8	71.1		0.111
31,32	2.0	7.5	75.6		0.126
33,34	4.0	1.5×10^{-3}	73.3		0.125
	Atm.	mol/l	μ sec	sec^{-1}	

$k(I) = 4.86 \times 10^7$

$k(II) = 8.41 \times 10^7$

A 10.4

$CH_3Cl + OH = CH_3Cl + H_2O$; t = 72°C Biomat/821001/8778.

run nr	p(CH_3Cl)	(CH_3Cl)	τ	dlnA/dt	A_{max}
27,28	$1.0x10^{-3}$	$3.53x10^{-5}$	71.1	$4.819x10^{3}$	0.121
29,30	$1.0x10^{-2}$	$3.53x10^{-4}$	22.2	$3.36x10^{4}$	0.108
31,32	1.5	5.30	16.4	4.22	0.096
33,34	2.5	8.83	10.0	7.25	0.084
36,37	$2.0x10^{-3}$	$7.06x10^{-5}$	55.6	$9.50x10^{3}$	0.131
	Atm.	mol/l	τ sec	sec^{-1}	

$k(I) = 6.86x10^{7}$

$k(II) = 8.03x10^{7}$

A 10.4

$CH_3Cl + OH = CH_2Cl + H_2O$; t = 100°C Biomat/821014/5242.

run nr	p(CH_3Cl)	(CH_3Cl)	τ	dlnA/dt	A_{max}
16,17	0	0	85.5		0.112
18,19	5.1×10^{-3}	1.7×10^{-4}	34.5	2.30×10^{4}	0.092
20,21	5.1	1.7	28.4	2.62	0.108
22,23	1.1×10^{-2}	3.7	15.6	5.24	0.095
24,25	2.1	6.9	8.9	7.49	0.119
26	4.2	1.4×10^{-3}	4.6	1.61×10^{5}	0.098
	Atm.	mol/l	μ sec	sec^{-1}	

$k(I) = 1.04 \times 10^{7}$

$k(II) = 1.10 \times 10^{7}$

A 10.4

$CH_3Cl + OH = CH_2Cl + H_2O$; t = 127°C Biomat/821018/1362.

run nr	$p(CH_3Cl)$	(CH_3Cl)	τ	dlnA/dt	A_{max}
25,26	0	0	91.0		0.119
27,28	0	0	77.5		0.116
29,30	0	0	64.5		0.119
31,32	3.3×10^{-3}	1.0×10^{-4}	39.5	1.66×10^{4}	0.112
33,34	8.7	2.6	19.3	3.64	0.112
35,36	2.0×10^{-2}	6.1	11.0	8.29	0.098
	Atm.	mol/l	μ sec	sec^{-1}	

$k(I) = 9.08\times10^{8}$

$k(II) = 1.31\times10^{8}$

A 10.5

$CH_2Cl_2 + OH = CHCl_2 + H_2O$; t = 27°C Biomat/821012/9015.

run nr	$p(CH_2Cl_2)$	(CH_2Cl_2)	τ	dlnA/dt	A_{max}
39,40	0	0	133.3		0.110
44	0	0	117.8		0.124
45,46	6.6×10^{-3}	2.67×10^{-4}	15.6	4.84×10^{4}	0.088
47,48	2.7	1.10	30.8	2.27	0.103
49,50	1.3	5.78×10^{-5}	54.4	6.83×10^{3}	0.115
	Atm.	mol/l	μ sec	sec^{-1}	

$k(I) = 1.46\times10^{8}$

$k(II) = 1.9\times10^{8}$

A 10.5

$CH_2Cl_2 + OH = CHCl_2 + H_2O$; t = 48°C Biomat/82!013/2274.

run nr	$p(CH_2Cl_2)$	(CH_2Cl_2)	τ	dlnA/dt	A_{max}
51,52	0	0	110.0		0.105
53	3.8×10^{-3}	1.4×10^{-4}	28.0	3.00×10^{4}	0.084
54,55	3.8	1.4	22.8	3.38	0.092
56,57	7.3	2.8	15.2	5.82	0.080
58,59	2.0	7.6×10^{-5}	38.4	1.78	0.106
	Atm.	mol/l	μ sec	sec^{-1}	

$k(I) = 1.42 \times 10^{8}$

$k(II) = 2.01 \times 10^{8}$

A 10.5

$CH_2Cl_2 + OH = CHCl_2 + H_2O$; t = 75°C Biomat/821001/1743.

run nr	$p(CH_2Cl_2)$	(CH_2Cl_2)	τ	dlnA/dt	A_{max}
3,4,7	0	0	113.0		0.117
8,9,10	4.8×10^{-3}	1.68×10^{-4}	20.0	2.8860×10^{4}	0.116
11,12	11.8×10^{-2}	4.13	11.0	6.6128	0.094
13,14	3.0×10^{-3}	1.01	32.8	1.9850	0.109
15,16	1.3	4.55×10^{-5}	40.0	1.3331	0.110
17,18	10.25×10^{-2}	3.59×10^{-4}	11.7	7.7258	0.107
19,20	10.25	3.59	11.7		0.120
21,22	0	0	55.6		0.118
23,24	0	0	58.9		0.119
	Atm	mol/l	μ sec	sec^{-1}	

$k(I) = 1.37 \times 10^{8}$

$k(II) = 2.04 \times 10^{8}$

A 10.5

$CH_2Cl_2 + OH = CHCl_2 + H_2O$; t = 100°C Biomat/821014/5242.

run nr	$p(CH_2Cl_2)$	(CH_2Cl_2)	τ	dlnA/dt	A_{max}
39,40	0	0	114.5		0.106
41,42	2.3×10^{-3}	7.6×10^{-5}	32.7	2.50×10^{4}	0.108
43,44	4.9	1.6×10^{-4}	17.9	4.32	0.111
46	6.7	2.2	14.6	5.92	0.104
47,48	9.1	3.0	11.0	6.19	0.106
	Atm.	mol/l	μ sec	sec^{-1}	

$k(I) = 1.89 \times 10^{8}$

$k(II) = 1.73 \times 10^{8}$

A 10.5

$CH_2Cl_2 + OH = CHCl_2 + H_2O$; t = 127°C Biomat/821018/1362.

run nr	$p(CH_2Cl_2)$	(CH_2Cl_2)	τ	dlnA/dt	A_{max}
37,38	0	0	81.0		0.120
39,40	3.6×10^{-3}	1.1×10^{-4}	24.8	2.88×10^{4}	0.117
41,42	5.8	1.8	16.7	5.76	0.109
43,44	1.4×10^{-2}	4.3	8.3	1.18×10^{5}	0.095
	Atm.	mol/l	μ sec	sec^{-1}	

$k(I) = 1.76 \times 10^{8}$

$k(II) = 2.72 \times 10^{8}$

A 10.6

F-22 + OH; t = 27°C Biomat/821011/5029.

run nr	p(F-22)	(F-22)	τ	dlnA/dt	A_{max}
56,57	0	0	183.3		0.119
58,59	1.2×10^{-2}	4.9×10^{-4}	128.0	5.32×10^{3}	0.092
61,62	2.0	8.14	103.0	6.01	0.081
63,64	3.2	1.3×10^{-3}	72.0	6.69	0.073
65,66	3.2	1.3	47.4	6.91	0.082
67,68	4.0	1.6	59.4	1.01×10^{4}	0.088
69.70	5.1	2.1	30.6	1.13	0.079
	Atm.	mol/l	μ sec	sec^{-1}	

$k(I) = 4.3 \times 10^{6}$

$k(II) = 4.2 \times 10^{6}$

A 10.6

F-22 + OH; t = 54°C Biomat/821025/5236.

run nr	p(F-22)	(F-22)	τ	dlnA/dt	A_{max}
23,24	0	0	164.0		0.129
25,26	2.0×10^{-2}	7.6×10^{-4}	87.0	6.80×10^{3}	0.104
27,28	3.9	1.4×10^{-3}	52.4	9.70	0.109
29,30	6.4	2.4	29.0	1.46×10^{4}	0.104
31	10.0	3.7	27.2	2.30	0.098
	Atm.	mol/l	μ sec	sec^{-1}	

$k(I) = 6.24 \times 10^{6}$

$k(II) = 5.25 \times 10^{6}$

A 10.6

F-22 + OH; t = 76°C Biomat/821025/5236.

run nr	p(F-22)	(F-22)	τ	dlnA/dt	A_{max}
1,2	0	0	66.5		0.121
11,12	2.1×10^{-2}	7.3×10^{-4}	59.5	9.64×10^{3}	0.111
13,14	5.1	1.8×10^{-3}	31.8	1.66×10^{4}	0.103
15,16	10.6	3.7	18.4	2.92	0.109
	Atm.	mol/l	μ sec	sec^{-1}	

$k(I) = 6.4 \times 10^{6}$

A 10.6

F-22 + OH; t = 105°C Biomat/821021/9929.

run nr	p(F-22)	(F-22)	τ	dlnA/dt	A_{max}
6,7	0	0	197.0		0.114
8,9	1.0×10^{-2}	3.2×10^{-4}	80.0	9.88×10^{3}	0.119
10	2.0	6.5	53.3	9.87	0.121
11,12	2.0	6.5	31.1	9.78	0.124
13,14	4.0	1.3×10^{-3}	36.1	1.52×10^{4}	0.115
15	8.0	2.6	21.1	3.05	0.114
17,18	16.0	5.2	15.0	4.06	0.100
19,20	0	0	108.0		0.121
21	0	0	100.0		0.115
	Atm.	mol/l	μ sec	sec^{-1}	

$k(I) = 7.56 \times 10^{6}$

$k(II) = 8.0 \times 10^{6}$

A 10.6

F-22 + OH; t = 127°C Biomat/821020/7208.

run nr	p(F-22)	(F-22)	τ	dlnA/dt	A_{max}
2,3	0	0	62.0		0.123
4,5	1.0×10^{-2}	3.1×10^{-4}	46.5	8.46×10^{3}	0.112
6	5.5	1.7×10^{-3}	25.0	2.97×10^{4}	0.090
7,8	5.5	1.7	20.0	3.95	0.109
10	8.1	2.5	17.8	4.41	0.098
11,12	0	0	89.0		0.127
14,15	2.3	7.1×10^{-4}	34.5	1.97×10^{4}	0.106
16,17	2.3	7.1	27.7	2.18	0.128
18,19	8.9	2.7×10^{-3}	11.4	5.45	0.096
20,21	0	0	108.5		0.115
	Atm.	mol/l	μ sec	sec^{-1}	

$k(I) = 1.50 \times 10^{7}$

$k(II) = 1.70 \times 10^{7}$

A 10.7

$CHCl_3 + OH = CCl_3 + H_2O$; t = 27°C Biomat/821012/9015.

run nr	$p(CHCl_3)$	$(CHCl_3)$	τ	dlnA/dt	A_{max}
3,4	0	0	104.0		0.102
6,7	0	0	128.0		0.105
8	0	0	115.8		0.109
14,15	0	0	117.2		0.121
16,17	1.6×10^{-4}	6.5×10^{-6}	121.0	5.29×10^{3}	0.122
18,19	1.3×10^{-3}	5.29×10^{-5}	59.0	7.28	0.109
20,21	9.5	3.87×10^{-4}	9.0	7.30×10^{4}	0.056
22,23	8.8	3.58	7.2	6.77	0.058
24	4.6	1.87	14.4	4.06	0.077
25	2.9	1.18	26.7	2.30	0.079
26,27	0	0	121.0	4.32	0.120
28	2.5	1.02	24.4	2.07	0.064
	Atm.	mol/l	μ sec	sec^{-1}	

$k(II) = 1.83 \times 10^{8}$

A 10.7

$CHCl_3 + OH = CCl_3 + H_2O$; t = 48°C Biomat/821013/2274.

run nr	p($CHCl_3$)	($CHCl_3$)	τ	dlnA/dt	A_{max}
61	0	0	127.8		0.103
62,63	1.6×10^{-3}	6.1×10^{-5}	48.5	1.44×10^{4}	0.091
64,65	3.0	1.1×10^{-4}	26.7	2.50	0.097
66,67	5.8	2.2	15.4	5.83	0.078
	Atm.	mol/l	μ sec	sec^{-1}	

$k(I) = 1.83 \times 10^{8}$

$k(II) = 2.81 \times 10^{8}$

A 10.7

$CHCl_3 + OH = CCl_3 + H_2O$; t =72°C Biomat/821001/8778.

run nr	$p(CHCl_3)$	$(CHCl_3)$	τ	dlnA/dt	A_{max}
38,39	0	0	80.0		0.112
40,41	4.0×10^{-3}	1.41×10^{-4}	27.8	3.51×10^{4}	0.090
42,43	2.5	8.83×10^{-5}	39.6	1.61	0.099
44,45	8.4	2.96×10^{-4}	7.6	8.35	0.080
	Atm.	mol/l	μ sec	sec^{-1}	

$k(I) = 2.27 \times 10^{8}$

A 10.7

$CHCl_3 + OH = CCl_3 + H_2O$; t = 100°C Biomat/821014/5242.

run nr	$p(CHCCl_3)$	$(CHCCl_3)$	τ	dlnA/dt	A_{max}
59,60	0	0	84.4		0.106
61,62	2.1×10^{-3}	6.9×10^{-5}	33.6	2.16×10^{4}	0.114
63,64	5.7	1.9×10^{-4}	16.3	4.82	0.094
65,66	9.1	3.0	11.3	6.01	0.113
	Atm.	mol/l	μ sec	sec^{-1}	

$k(I) = 1.78 \times 10^{8}$

$k(II) = 1.68 \times 10^{8}$

A 10.7

$CHCl_3 + OH = CCl_3 + H_2O$; t = 127°C Biomat/821018/1362.

run nr	p($CHCl_3$)	($CHCl_3$)	τ	dlnA/dt	A_{max}
45,46	0	0	105.6		0.118
47,48	2.0×10^{-3}	6.1×10^{-5}	36.0	1.80×10^{4}	0.097
49,50	3.6	1.1×10^{-4}	24.2	3.34	0.092
51,52	7.4	2.3	25.0	6.48	0.090
	Atm.	mol/l	τ	sec^{-1}	

$k(I) = 2.17 \times 10^{8}$

$k(II) = 2.82 \times 10^{8}$

A 10.8

$CH_3CCl_3 + OH = CH_2CCl_3 + H_2O$; t = 27°C Biomat/821012/9015.

run nr	$p(CH_3CCl_3)$	(CH_3CCl_3)	τ	dlnA/dt	A_{max}
51,52	0	0	134.4		0.134
53,54	2.2×10^{-3}	8.9×10^{-5}	22.4	2.50×10^{4}	0.092
55,56	1.1	4.5	31.6	1.77	0.102
57,58	1.1	4.5	26.2	2.25	0.097
59,60	4.0	1.62×10^{-4}	10.8	5.34	0.083
	Atm.	mol/l	μ sec	sec^{-1}	

$k(I) = 3.64\times10^{8}$

$k(II) = 3.50\times10^{8}$

A 10.8

$CH_3CCl_3 + OH = CH_2CCl_3 + H_2O$; t = 48°C Biomat/821013/2274.

run nr	$p(CH_3CCl_3)$	(CH_3CCl_3)	τ	dlnA/dt	A_{max}
68,69	0	0	83.2		0.110
70,71	1.4×10^{-3}	5.1×10^{-5}	40.8	1.19×10^{4}	0.109
72,73	2.5	9.5	30.2	2.28	0.092
74,75	4.9	1.8×10^{-4}	20.8	4.37	0.080
	Atm.	mol/l	μ sec	sec^{-1}	

$k(I) = 1.34\times10^{8}$

$k(II) = 2.39\times10^{8}$

$CH_3CCl_3 + OH = CH_2CCl_3 + H_2O$; t = 75°C Biomat/821005/4648.

run nr	$p(CH_3CCl_3)$	(CH_3CCl_3)	τ	dlnA/dt	A_{max}
1,2	0	0	58.9		0.125
3.4	0	0	80.0		0.122
5.6	0	0	83.3		0.116
7,8	0	0	88.0		0.118
9,10,11	0	0	121.0		0.096
12,13	0	0	84.4		0.119
14,15	3.0×10^{-3}	1.1×10^{-4}	27.5	2.53×10^{4}	0.118
16,17	5.8	2.03	16.4	4.51	0.105
20,21	8.0	2.8	13.3	5.76	0.098
22,23	8.9×10^{-2}	3.1×10^{-3}	4.2	2.07×10^{5}	0.050
24,25	3.1	1.1	5.6	1.30	0.067
26,27	1.5	$5,4\times10^{-4}$	7.6	1.15	0.102
28	1.5	5.4	17.1	2.04×10^{4}	0.096
30	0	0	15.8		0.090
31	0	0	31.0		0.079
35,36	0	0	82.2		0.121
37,38	1.7×10^{-3}	6.0×10^{-5}	41.1	1.51×10^{4}	0.111
39	1.7	6.0	45.0	1.64	0.099
40,41	3.0	1.1×10^{-4}	27.5	2.86	0.105
42,43	4.9	1.7	17.4	4.04	0.106
44,45	7.4	2.6	12.5	6.22	0.099
49,50	2.6×10^{-2}	9.2	6.7	1.03	0.083
	Atm.	mol/l	μ sec	sec^{-1}	

$k(I) = 2.26\times10^{8}$
$k(II) = 2.09\times10^{8}$

A 10.8

$CH_3CCl_3 + OH = CH_2CCl_3 + H_2O$; t = 100°C Biomat/821014/5242.

run nr	$p(CH_3CCl_3)$	(CH_3CCl_3)	τ	dlnA/dt	A_{max}
49,50	0	0	117.2		0.106
51,52	2.1×10^{-3}	6.9×10^{-5}	29.6	1.88×10^{4}	0.103
53,54	4.0	1.3×10^{-4}	19.0	3.29	0.107
55,56	6.9	2.3	14.2	5.76	0.088
57,58	8.6	2.8	10.4	6.01	0.115
	Atm.	mol/l	μ sec	sec^{-1}	

$k(I) = 2.01 \times 10^{8}$

$k(II) = 1.95 \times 10^{8}$

A 10.8

$CH_3CCl_3 + OH = CH_2CCl_3 + H_2O$; t = 127°C Biomat/821018/1362.

run nr	$p(CH_3CCl_3)$	(CH_3CCl_3)	τ	dlnA/dt	A_{max}
53	0	0	62.2		0.105
54,55	0	0	105.6		0.099
56,57	1.6×10^{-3}	4.9×10^{-5}	33.0	1.84×10^{4}	0.094
58,59	3.1	9.5	23.0	2.92	0.107
	Atm.	mol/l	μ sec	sec^{-1}	

$k(I) = 2.50\times10^{8}$

$k(II) = 2.36\times10^{8}$

A 10.8

$CH_3CCl_3 + OH = CH_2CCl_3 + H_2O$; t = 127°C Biomat/821020/7208.

run nr	$p(CH_3CCl_3)$	(CH_3CCl_3)	τ	dlnA/dt	A_{max}
22,23	5.8×10^{-3}	1.8×10^{-4}	11.6		0.105
24,25	5.5	1.7	15.7		0.116
26,27	3.2	9.8×10^{-5}	32.1		0.114
28,29	3.0	9.2	25.7		0.110
	Atm.	mol/l	μ sec	sec^{-1}	

22,23,28,29 Fluka

24,25,26,27 Renseværksted

Risø National Laboratory **Risø - M - 2366**

Risø - M -

Title and author(s)

Kinetics of the Reaction of Hydroxyl Radicals with Ethane and a series of Cl- and F-substituted Methanes at 300-400°K. OH as a Tropospheric Sink preventing Ozone Depletion

Erik Bjarnov, Jette Munk, Ole John Nielsen, Palle Pagsberg, and Alfred Sillesen

Date: April 1983

Department or group: Chemistry Dept.

Group's own registration number(s):

133 pages + tables + illustrations

Abstract

Gas phase reactions of hydroxyl radicals with ethane and a series of Cl- and F-substituted methanes were studied at atmospheric pressure and over the temperature range 300-400°K. Hydroxyl radicals were produced by pulse radiolysis of water vapour and the decay rate was studied by monitoring the transient light absorption at 3090 Å. Arrhenius parameters (A, E_a) for the reaction RH + OH -> R + HOH were obtained for the reactants RH = C_2H_6, CH_3Cl, CH_2Cl_2, $CHFCl_2$. CF_2Cl_2 (CFC-12) which contains no C-H bonds was found to be inert toward attack by hydroxyl radicals. Since no other tropospheric sink reactions have been reported for CFC-12 its possible impact on the stratospheric ozone remains a controversial problem.

Copies to

Available on request from Risø Library, Risø National Laboratory (Risø Bibliotek), Forsøgsanlæg Risø), DK-4000 Roskilde, Denmark
Telephone: (02) 37 12 12, ext. 2262. Telex: 43116